

الجمهورية الجزائرية الديمقراطية
الشعبية

PEOPLE'S DEMOCRATIC REPUBLIC OF ALGERIA

وزارة التعليم العالي والبحث
العلمي

MINISTRY OF HIGHER EDUCATION AND SCIENTIFIC RESEARCH

جامعة أبي بكر بلقايد - تلمسان

ABOUBAKR BELKAID UNIVERSITY – TLEMCEM – FACULTY OF
TECHNOLOGY



THESIS

Presented for obtaining the Master's degree

In: Mechanical engineering

Specialty: Energetics

By: Benosman Lotfi and Sebaihi Tani Ryad

Subject

Numerical simulation of a double pass solar air collector

Publicly defended 19/06/2025, In front of the jury composed of

Mr Saim Rachid	Pr	University of Tlemcen	President
Mr Benmansour Abdelkarim	MCB	University of Tlemcen	Examiner
Mr Korty Nabil Abdelilah	Professor	University of Tlemcen	Supervisor
Mme Khaldi Souhila	MCB	University of Tlemcen	Co-supervisor

Academic year: 2024/2025

Acknowledgements

First and foremost, I express my deepest gratitude to Allah, the Most Gracious and the Most Merciful, for granting me the strength, patience, and determination to complete this work.

I would like to extend my sincere thanks to my supervisor, Dr. Korti Abdelillah Nabil, for his continuous guidance, encouragement, and valuable insights throughout this research. His support and expertise have been truly instrumental in the development of this thesis.

My heartfelt appreciation also goes to my co-supervisor, Dr. Khaldi Souhila, whose attentive supervision, helpful feedback, and kind encouragement helped me stay on the right track during every stage of this work.

I also wish to thank the members of the jury, Dr. Saim Rachid and Dr. Benmansour Abdelkarim, for accepting to evaluate this thesis and for their valuable comments and recommendations, which have enriched the final version of this work.

I would especially like to express my profound gratitude to DR Benazzouz Rabia. Her exceptional dedication, insightful advice, and unwavering support have had a significant impact. Her encouragement and kindness were a constant source of motivation, and I am deeply thankful for the time and effort she generously devoted to my academic progress.

To all who have supported me during this academic journey, directly or indirectly, I extend my sincere thanks.

Dedication

To my beloved parents,

Your unwavering love, endless sacrifices, and constant prayers have been the foundation of everything I have achieved. This work is a reflection of your strength and support. Thank you for always believing in me.

To my dear brothers,

Thank you for your encouragement, your patience, and for always being there with a kind word and a helping hand. Your support means more than words can express.

To my cherished family,

Your presence in my life has been a constant source of motivation and comfort. I deeply appreciate your love and support every step of the way

To my dear friends,

Your companionship, understanding, and encouragement throughout this journey have been truly invaluable. Thank you for walking this path with me and lifting my spirits when I needed it most.

This thesis is dedicated to all of you — with love and gratitude.

Lotfi and Ryad

المخلص

تُساهم التطورات الحالية في مجال الطاقات المتجددة وأدوات المحاكاة الحاسوبية بشكل كبير في نمذجة وتحسين أنظمة تحويل الطاقة، مما يتيح اختيارًا دقيقًا للمكونات وتكيفًا أفضل مع الاستخدامات الصناعية والمنزلية المتنوعة. يركز هذا العمل على برمجة وتطوير نموذج محاكاة للأداء الحراري لمجمع شمسي مسطح لتسخين الهواء باستخدام برنامج MATLAB. تسلط هذه الدراسة الضوء على الإطار النظري، منهجية النمذجة، وعملية التحقق من الأداء الحراري للمجمع الشمسي من خلال المحاكاة العددية. وتوفر النتائج تحليلًا تفصيليًا لكفاءة النظام في ظروف تشغيل مختلفة، مما يبرز إمكانياته كحل طاقة مستدامة

الكلمات المفتاحية : محاكاة ، الأداء الحراري، الطاقات المتجددة، النمذجة العددية MATLAB،

Abstract

The current advancements in the field of renewable energy and computational tools greatly assist in the simulation and optimization of energy conversion systems, enabling the precise selection of components and better adaptation to diverse industrial and domestic applications. The programming and development of a simulation model for the thermal performance of a flat-plate solar air collector using MATLAB is the central focus of this work. This study highlights the theoretical framework, modeling approach, and validation process for the thermal performance of the solar air collector through numerical simulations. The results provide a detailed analysis of the system's efficiency under various operating conditions, emphasizing its potential for sustainable energy solutions.

Keywords: Flat-plate solar air collector, renewable energy, thermal performance, MATLAB simulation, numerical modeling.

Résumé

Les progrès actuels dans le domaine des énergies renouvelables et des outils de simulation informatique contribuent grandement à la modélisation et à l'optimisation des systèmes de conversion d'énergie, permettant une sélection précise des composants et une meilleure adaptation à divers usages industriels et domestiques. La programmation et le développement d'un modèle de simulation des performances thermiques d'un capteur solaire plan à air à l'aide de MATLAB constituent le sujet central de ce travail. Cette étude met en avant le cadre théorique, l'approche de modélisation et le processus de validation des performances thermiques du capteur solaire grâce à des simulations numériques. Les résultats fournissent une analyse détaillée de l'efficacité du système dans différentes conditions de fonctionnement, soulignant son potentiel pour des solutions énergétiques durables.

Mots-clés : Capteur solaire plan à air, énergies renouvelables, performances thermiques, simulation MATLAB ,modélisation numérique.

Table of contents

Chapter I Generalities on Solar Radiation and Solar Collectors	13
I.1. Introduction.....	14
I.2. Solar field in Algeria.....	14
I.3. Different modes of thermal transfer:.....	16
I.3.1. Conduction	16
I.3.2. Convection	16
I.3.3. Natural convection	16
I.3.4. Radiation	17
I.4. types of solar collectors	18
I.4.2. Thermal Solar Collectors definition	18
I.4.3. Different Types of Solar Thermal Collectors	20
I.5. Flat plate solar air collectors	26
I.5.1. Flat plate solar air collectors definition	26
I.5.2. Role of each component.....	26
I.5.3. Parameters and Operating Characteristics of Solar Collectors	32
I.5.4. Applications of Flat-Plate Solar air Collector	33
I.6. conclusion	35
Chapter II Literature review	36
II.1. introduction:.....	37
II.2. Finned absorber plate:	37
II.3. Absorber with baffles and obstacles	40
II.4. Other competent improvements of flat plate solar air collector	42
II.5. Thermal insulation:.....	45
II.6. Thermal energy storage:	45
Chapter III	48
III.1. Introduction	49
III.2. Description of The flat-plate solar collector.....	49
III.3. Mathematical modelling:.....	51
III.4. Evaluation of Thermal Coefficients and Dimensionless Numbers	52
III.4.1. Thermal transfer by convection	52
III.4.2. Thermal transfer by radiation	53
III.5. Overall thermal balance of a flat plate air collector in transient state:.....	54
III.5.1. Analytical expressions for energy balance	54

III.5.2. boundary conditions	56
III.5.3. thermal efficiency	57
III.5.4. The physical properties.....	57
III.6. Numerical Modelling	57
III.6.1. Principle of the Finite Difference Method (FDM)	58
III.6.2. The General Algorithm:.....	61
III.7. Analysis of diurnal variation of solar radiation on ambient temperature:.....	61
III.8. Conclusion.....	62
Chapter IV	63
IV.1. Introduction:	64
IV.2. Temperature evaluation in the solar collector.....	64
IV.3. Spatial temperature evolution of air through the collector	65
IV.4. Effect of mass flow rate on fluid temperatures as a function of distance:.....	66
IV.5. Effect of solar radiation on fluid temperatures as a function of distance	67
IV.6. Effect of Mass Flow Rate and Solar Radiation on Fluid Temperatures as a Function of Time.....	68
IV.6.1. Effect of masse flow rate	68
IV.6.2. Effect of solar intensity	69
IV.7. Thermal efficiency.....	71
IV.7.1. Temporal Variation of Thermal Efficiency	71
IV.7.2. Impact of mass flow rate on thermal efficiency.....	72
IV.7.3. Impact of solar intensity on thermal efficiency	73
IV.7.4. Conclusion	74
IV.8. General conclusion :	74

Liste of figures

Chapter I

Figure I.1: World map of global horizontal irradiation	14
Figure I.2:average annual sunshine duration in hours.....	15
Figure I.3:Flat based air solar collector.....	19
Figure I.4:Image showing a solar water heater	19
Figure I.5 : Glazed Flat Plate solar Collector	21

Figure I.6: heat transfer phenomena	21
Figure I 7: Unglazed Flat-Plate Collectors.....	22
Figure I.8 Unglazed flat plate solar collector for used for pool heating	23
Figure I.9 : Vacuum tube solar collector	24
Figure I.11:Cylindrical-Parabolic Collector.....	24
Figure I.12 Parabolic reflector system	25
Figure I.13 solar power tower	25
Figure I.14 : solar air heater	26
Figure I.15: Schematic view of the indirect type solar drye	33
Figure I.16: Solar collector used for air conditioning.....	33
Figure I.17: The Trombe-Michel Wall	34

Chapter II

Figure II.1: Solar v-groove air collector	37
Figure II.2: Air heater with herringbone corrugated fins with geometrical description	38
Figure II.3: Schematic diagram of double pass solar air heater with (a) fins and (b) fins with baffles.	39
Figure II.4: Absorber plate configurations (a. flat plate, b.pin fins, c.corrugated fins, and d. corrugated-perforated fins	39
Figure II.5: (a) installation of solar drying system (b) Directions of fins on the absorbing surfaces of collectors (c) Design of drying chamber.....	40
Figure II.6: Geometry of designed solar collectors; a) PPSC, b) PPSCB, c) PPSCDB.....	41
Figure II.7: Illustrative lateral view of the internal convection flow of the solar collector without barrier (A) and with Barrier (B).	42
Figure II.8: The experimental setup (front view).....	43
Figure II.9: The absorber of the TSAH.....	43
Figure II.10: .Experimental Setup (a) flat plate collector - with 45° inclination, (b) flat plate collector with reflectors, (c) flat plate collector with Black Chrome coating, (d) flat plate collector with nickel cobalt coating.....	44
Figure II.11: Experimental set up.....	44
Figure II.12: Photo of the solar air collector	45
Figure II.13: soalr dryer with heat storage	46
Figure II.14: Solar air heater integrated with drying cabinets	47

Chapter III

Figure III.1: Schematic Diagram of the Flat-Plate Solar Air Collector.	49
Figure III.3: Thermal exchanges between the components of a flat plate solar air collector." 51	
Figure III.4: The Principle of Numerical Calculation.....	58
Figure III.5: Meshing for Numerical Calculation	60
Figure III.6: Flowchart of the Numerical Calculation.....	60
Figure III.7: Diurnal variation of average solar radiation on ambient temperature.....	62

Chapter IV

Figure IV.1: temporal evolution of the temperatures of various components of the solar collector	64
Figure IV.2 variation of fluid temperature along a double-pass collector.	65
Figure IV.3: the effect of mass flow rate on the variation of fluid temperatures with different values of masse flow mf [0,01 0,02 0,03 kg/s]	66
Figure IV.4: The effect of solar radiation on the variation of fluid temperatures with different values of solar radiation It[700 850 1000]	67
Figure IV.5: the impact of the mass flow rate on the outlet fluid temperature in a solar collector	68
Figure IV.6: The impact of solar intensity on the outlet temperature of the fluid in a solar collector	70
Figure IV.7: Temporal Variation of Thermal Efficiency	72
Figure IV.8: impact of mass flow rate on thermal efficiency	72
Figure IV.9: impact of solar radiation on thermal efficiency	73

Tables liste

Table I.1: Solar potential in Algeria	15
Table I.2: Advantages and disadvantages of glazed flat-plate collectors	21
Table I.3: Advantages and disadvantages of unglazed flat-plate collectors.	23
Table I.4 characteristics of materials used as absorbers.....	28
Table I.5: Absorption, reflectivity, and emissivity of different surface colors	29
Table I.6: Thermal caracteristiques of absorber materials.....	30

Table I.8: Thermal properties of some insulating material..... 31

Table III.1: geometrical parameters of the collector 50

Table III.2: Numerical Schemes of Partial Derivative 59

NOMENCLATURE

A: surface area (m^2)

C_p: specific heat ($kJ/kg.k$)

D_h: Hydraulic diameter (m)

m_r: Air mass flow rate (kg/s)

h_r: Radiative heat transfer coefficient ($W/m^2.K$)

h_c: Convective heat transfer coefficient ($W/m^2.K$)

U: overall heat loss coefficient. ($W/m^2.K$)

I_t: Total radiation flux received by the air collector (W/m^2)

q : Heat transfer rate

K: Thermal conductivity ($W/m \cdot K$)

T: Temperature (K)

ΔT: temperature difference (K)

V : velocity (m/s)

m: mass (kg)

e: Thickness (m)

h : Convective heat transfer coefficient due to wind ($W/m^2.K$)

FDM: The finite difference method

Dimensionless Numbers

Re: Reynolds number

Pr: Prandtl number

Nu: Nusselt number

Greek Letters

α : Absorptivity coefficient

ε : Emissivity

τ : Transmissivity coefficient

μ : dynamic viscosity

ρ : density (kg/ m³)

η : thermal efficiency

σ : Stefan-Boltzmann Constant (5.67×10^{-8}) (W/m² K⁴)

Subscripts

p: Absorber

g: glass cover

w: wind

f1: Fluid in the first passage

f2: Fluid in the second passage

b: Insulation

f1-b: first pass fluid to insulation

g-amb: glass cover to ambient air

g-f2: glass cover to air stream-II

g-sky: glass cover to sky

f1-p : first pass fluid to absorber

p-g : absorber to glass cover

f2-p : second pass fluid to absorber

p-sky: absorber to sky

GENERAL INTRODUCTION

Energy has always been a vital issue for humanity and human societies, profoundly influencing behavior based on its availability, abundance, or scarcity. Conventional energy sources such as coal, oil, natural gas, and uranium have served as essential pillars of our industrial society, yet their finite nature contrasts with renewable energies like solar, wind, and hydropower, which are inexhaustible and environmentally friendly. The exploitation of fossil fuels not only depletes these limited resources but also generates significant carbon dioxide (CO₂) emissions, contributing to global warming and climate change. According to the World Meteorological Organization's 2023 Greenhouse Gas Bulletin, atmospheric CO₂ concentrations have increased by 11.4 % over the past 20 years [1], further highlighting the urgent need for sustainable energy solutions.

As the world economy continues to expand, population growth has amplified the demand for electricity, space heating and cooling, food, and consumer products. Over the past decade, global electricity consumption has increased at an average annual rate of 3%, reflecting the accelerating energy needs of modern societies.[2]

These environmental challenges have led to severe consequences such as droughts and floods, underscoring the necessity of global cooperation. Recognizing this, international efforts like the Kyoto Protocol in 1997 targeted reducing greenhouse gas emissions to limit global warming to below 2°C. This momentum was further reinforced by the 2015 Paris Agreement, which emphasized the necessity of keeping global temperature increases below 1.5°C to address fossil fuel depletion and mitigate environmental challenges[3]. These initiatives have driven many countries to adopt renewable energy sources, including wind, geothermal, and solar power.

Algeria, due to its geographical location, benefits from one of the highest solar resources in the world. The duration of sunshine across nearly the entire national territory exceeds 2,000 hours per year and can reach up to 3,900 hours in the high plateaus and the Sahara region. This abundant solar potential makes Algeria an ideal candidate for large-scale solar energy projects, furthering the global transition toward renewable energy. Solar energy, in particular, holds significant promise, with technologies like solar concentrators, vacuum solar collectors, and flat-plate collectors playing pivotal roles. Double-pass flat-plate collectors, for example, are designed to capture solar radiation and convert it into thermal energy. Such advancements highlight the critical role of renewable energy in addressing climate change and ensuring a sustainable future.

The objective of this work is to conduct a thermal study of a double-pass flat-plate solar air collector, aiming to simulate solar radiation and its thermal performance using the MATLAB environment.

Our thesis consists of four chapters:

The first chapter provides a general overview of solar collectors and the different types of these devices.

The second chapter is a literature review dedicated to presenting the research work on the field of solar air collectors and the development of different types of these devices.

The third chapter covers the physical and mathematical modeling of flat-plate solar collectors, including numerical solution.

The fourth chapter discusses the effects of mass flow rate and solar radiation on fluid temperatures, thermal efficiency, and presents the overall results and conclusions.

This study concludes with a general conclusion that summarizes the most significant results of the work

Chapter I
Generalities on Solar Radiation and
Solar Collectors

I.1. Introduction

The Sun is part of a stellar system containing about 340 billion stars, mostly concentrated in a disk-shaped region with arms extending from a central nucleus. It is located 28,000 light-years from the center, orbiting at 225 km/s [2], completing one revolution every 300 million years. As the central star of our planetary system, it has 7 planets, 5 dwarf planets, and millions of asteroids orbiting around it. The Sun holds more than 99.8% of the solar system's total mass[2]. It is composed of 75% hydrogen and 25% helium by mass, and 92.1% hydrogen and 7.8% helium by atomic number, with other elements accounting for less than 0.1%. These values gradually change as the Sun undergoes nuclear fusion, converting hydrogen into helium.[3]

Sun is as old as the universe itself and is a free and an inexhaustible source of energy.

The Sun is acknowledged as the largest source of renewable energy. Each second, it loses approximately 4.5×10^9 tons of material, which transforms into solar radiation. Only a small portion of this energy reaches Earth, estimated at 18×10^{13} kW, about 10,000 times the total global energy consumption per year. Annually, the energy potential from the Sun available to Earth is around 4×10^{17} kWh. [3]

With few exceptions, most countries of the developing world are located in climatic zones receiving reasonably higher insolation than the world average that varies from 1600 to 2200 kWh/m² /year [4]

The duration and intensity of sunlight vary based on the time of year, weather conditions, and geographic location. In areas within the "Sun Belt," annual global solar radiation on a horizontal surface can exceed 2,200 kWh/m²[5]

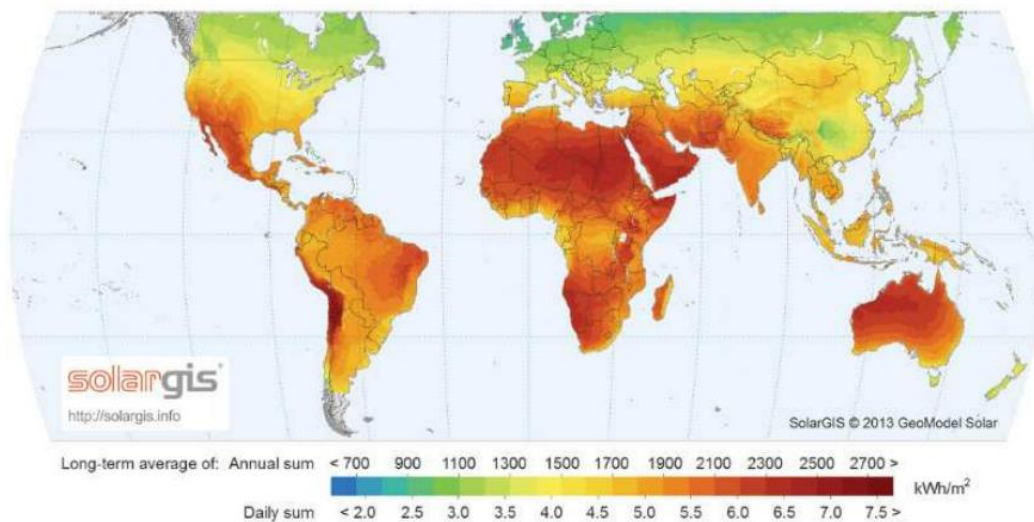


Figure I.1: World map of global horizontal irradiation [5]

I.2. Solar field in Algeria

The solar resource refers to a set of data describing the variation of available solar radiation over a given period. This data is crucial for simulating the performance of solar energy systems and accurately sizing them according to specific energy demands [6]

It finds application in a wide range of fields, including agriculture, meteorology, energy management, and public safety.

Due to its geographical location, Algeria benefits from one of the highest solar resources in the world, as illustrated in Figure. The duration of sunshine across nearly the entire national territory exceeds 2,000 hours per year and can reach up to 3,900 hours in the high plateaus and the Sahara region.[7]

The energy received daily on a horizontal surface of 1 m² averages around 5 kWh across most of the country. This corresponds to approximately 1,700 kWh/m²/year in the north and 2,263 kWh/m²/year in the south. Overall, Algeria's solar potential surpasses 5 billion GWh.[7]

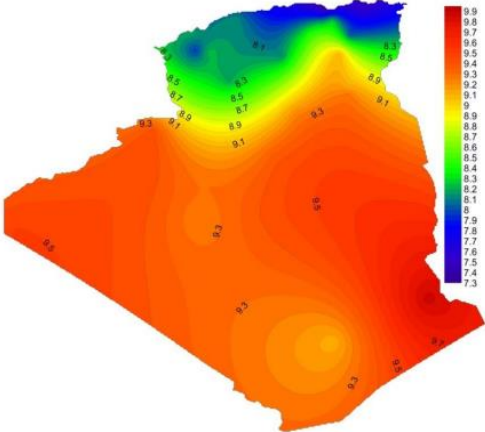


Figure I.2:average annual sunshine duration in hours (1983-2012)[7]

Algeria has one of the world's largest solar energy potentials, largely due to its desert climate and extensive sunlit areas, especially in the Sahara. With an average of 2500 hours of sunlight annually, the country is well-suited for solar energy production. This potential is estimated at approximately 169,440 TWh per year, far exceeding its own national electricity needs and about sixty times the European Union's annual energy consumption. Algeria could thus become a significant player in renewable energy exports, particularly to Europe, making it a strategic asset in the global energy transition [3] as shown in the table below.

Table I.1:Solar potential in Algeria [7]

Regions	Coastal Regions	High Plateaus	Sahara
Surface Area (%)	4	10	86
Average Sunshine Duration (h/year)	2650	3000	3500
Average Energy Received (kwh/m ² /year)	1700	1900	2650

Energy production and consumption in Algeria are predominantly based on petroleum products and natural gas, which account for 99% of the total. Renewable energies, such as solar power, contribute only 1%, with solar energy specifically representing 0.8% of this renewable production.[8]

The use of thermal solar energy is becoming increasingly relevant due to its substantial impact on reducing CO₂ emissions and the enhanced performance of installation. To harness or store solar energy, it must be converted into another form of energy. To achieve this, solar collectors are used.

The measurement of solar radiation in Algeria is carried out by the National Meteorological Office (O.N.M) through a network of 81 meteorological stations responsible for monitoring sunshine duration. However, between 1970 and 1989, only seven of these stations collected data on diffuse and global radiation components on a horizontal plane. It is worth noting that these data series contain gaps due to periods of instrument inactivity. By 2011, available information indicated that only three stations—located in Oran, Tamanrasset, and Ksar Chellala—regularly measured solar radiation on a horizontal plane.

Additionally, since 2009, eight more automatic stations have been operational for recording this data, including those in Algiers (airport), Oran (Sénia), In Amenas, Ghardaïa, Annaba, Tamanrasset, Tlemcen, and Constantine.[6]

I.3. Different modes of thermal transfer:

I.3.1. Conduction

is a mode of heat transfer that occurs within a material or between materials in direct contact when a temperature gradient exists without any movement of the material itself. This transfer happens through vibrations of particles, or the movement of free electrons, depending on the nature of the material [9]

$$q_x = -k A \frac{dT}{dx}$$

where

q_x : the heat-transfer rate (W)

k : Thermal conductivity of the material (W/m·K)

A : Heat transfer surface area (m²)

$\frac{dT}{dx}$: the temperature gradient in the direction of the heat flow

I.3.2. Convection

Convection is a mode of heat transfer that occurs through the movement of a fluid (liquid or gas). It involves the transport of heat from one region to another driven by temperature differences within the fluid [10]

I.3.3. Natural convection

Happens due to natural buoyancy forces. the warm and less dense fluid rises while cool and more dense fluid sinks ,this creates a circulation pattern

a. Forced convection

Heat transfer is aided by external forces such as a fan, pump, or blower that moves the fluid. To express the overall effect of convection, we use Newton's law :

$$q = h A (T_s - T_\infty)$$

where

q :Heat transfer rate (W)

h: Convective heat transfer coefficient (W/m²·K)

A: Surface area (m²)

T_s:Surface temperature (K or °C)

T_∞:Fluid temperature far from the surface (K or °C)

1.3.4. Radiation

Radiation heat transfer is the transfer of thermal energy through electromagnetic waves, without the need for a physical medium. This mode of heat transfer can occur in a vacuum and is governed by the emission, absorption, and reflection of electromagnetic radiation by surfaces.

$$q = \sigma \varepsilon A (T_1^4 - T_2^4)$$

where

q: Radiative heat transfer rate (W)

σ: Stefan-Boltzmann constant (5.67×10⁻⁸ W/m²·K⁴)

ε: Emissivity of the surface.

A: Surface area (m²)

T₁⁴, T₂⁴: temperatures of the two surfaces (K).

2 Solar Thermal Energy

- Principles of Solar Thermal Conversion

The primary function of a thermal solar collector is to convert solar radiation into usable thermal energy, often by heating a transfer fluid such as water or air. This conversion relies on the greenhouse effect: solar radiation passes through a transparent cover to reach an absorber surface, typically coated in black. The absorber captures most of the incoming radiation, raising its temperature. Infrared radiation emitted by the absorber is reflected back by the glass cover, which prevents heat loss by trapping these infrared rays within the system.[11]

- **blackbody**: blackbody refers to a material that absorbs all the light it receives, making it ideal for capturing solar radiation.
- **greenhouse effect**: greenhouse effect occurs when certain materials allow a wide range of wavelengths to pass through, while glass is transparent only to visible light and near-infrared radiation. By surrounding a blackbody with a glass enclosure, the light passing

through the glass heats the blackbody to temperatures between 30°C and 100°C. The blackbody, now emitting infrared radiation, is trapped by the glass, leading to further heating — this is the greenhouse effect.[11]

- Applications of Solar Thermal Energy in Heating Systems

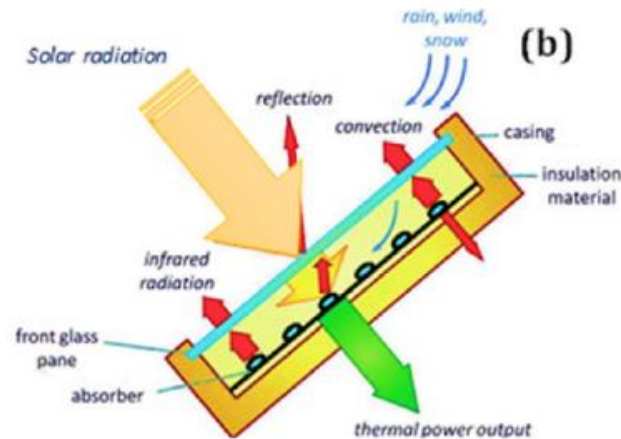


Figure I.3. Operating principle of a glazed flat-plate solar collector.

I.4. types of solar collectors

Based on energy conversion, two main types of solar collectors are distinguished:

a. Photovoltaic Solar panels

These convert solar radiation directly into electrical energy using photovoltaic cells

b. Thermal Solar Collectors

These convert solar radiation into thermal energy, primarily for heating purposes.

I.4.2. Thermal Solar Collectors definition

Thermal Solar Collectors are devices used to capture and convert sunlight into heat, typically for applications such as heating water, air, or for use in industrial processes. These collectors absorb solar radiation and transfer it to a fluid (usually water or air) that circulates through the system. The heated fluid is then used for space heating, domestic hot water, or other thermal applications.

thermal solar collectors can be classified based on temperature:

- **Low-temperature collectors:** Used for applications like water heating.
- **Medium-temperature collectors:** Used for space heating or industrial processes.
- **High-temperature collectors:** Typically used for power generation or specialized industrial applications requiring higher heat levels.

Each type of collector is designed to operate efficiently within its specific temperature range.[11]

Also, Solar collectors can be classified based on the working fluid used. Among these types, we find:

I.4.2.1. Air based solar collectors

These collectors are designed for use in air heating systems, particularly for drying agricultural products and heating buildings. [11]



Figure I.4:Flat based air solar collector

I.4.2.2. The Water-Based Solar Collector

There are primarily two types of circulation systems: low-pressure and high-pressure systems

- Low-pressure system: This system is commonly used for heating swimming pools, industrial water heating, and domestic heating purposes.
- High-pressure system: In this system, the water circuit typically consists of copper tubes combined with a metal plate, which increases the absorption surface. The fins, usually made of steel, aluminium, or copper, vary in thickness according to the thermal conductivity of the material: approximately 0.25 mm for copper, 0.5 mm for aluminium, and 2 mm for steel. The spacing between the tubes depends on the thickness of the fins.[12]



Figure I.5:Image showing a solar water heater [41]

I.4.3. Different Types of Solar Thermal Collectors

There are several types of solar thermal collectors, classified based on temperature: low temperature, medium temperature, and high temperature collectors [4].

there are mainly two types of solar thermal collectors:

- Flat plate collector.
- Concentrating collector.

I.4.3.1. Flat plate collectors

A flat plate solar collector is a device designed to capture the energy carried by solar radiation, convert it into thermal energy, and transfer it to a heat transfer fluid. It combines two physical principles: the greenhouse effect and the black body effect.

When solar radiation passes through a transparent cover and impinges on the blackened absorber surface of high absorptivity, a large portion of this energy is absorbed by the plate and transferred to the transport medium in the fluid tubes. [11]

There is a wide range of solar collectors available to meet different liquid heating needs. The choice of collector depends on the desired temperature and the climatic conditions during the system's usage period. Naturally, the higher the temperature level, the more advanced the technologies used, and the higher the production costs. The most common technologies for flat plate collectors are:

- Glazed flat plate collectors.
- Unglazed flat plate collectors.
- Vacuum tube flat plate collectors.

a. Glazed Flat Plate Collectors

A glazed flat plate solar collector is a very simple element, consisting of a metallic absorber that transforms solar radiation into heat and transfers this heat to a heat transfer fluid. This absorber is mounted in an insulated box, covered with highly transparent glass or synthetic material. The absorber has a black selective coating that effectively absorbs solar radiation.

For temperature levels from 35°C to 90°C, glazed collectors are required. In this case, the absorber is metallic (copper or aluminum), placed in an insulated box at the back, and covered with glazing at the front.

The transparent cover is used to reduce convection losses from the absorber plate through the restraint of the stagnant air layer between the absorber plate and the glass. It also reduces radiation losses from the collector as the glass is transparent to the short wave radiation received by the sun but it is nearly opaque to long-wave thermal radiation emitted by the absorber plate (greenhouse effect). [22]

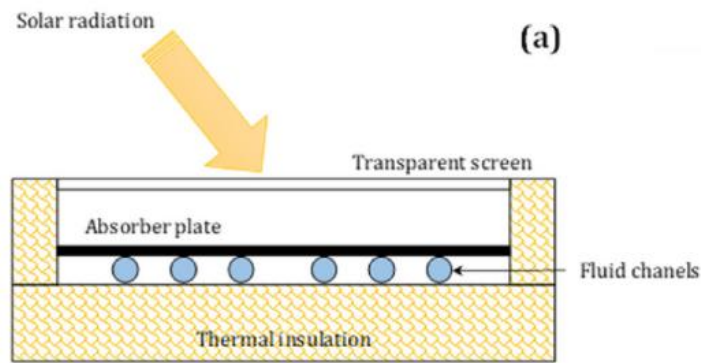


Figure I.6 : Glazed Flat Plate solar Collector

A portion of the solar radiation that reaches the glass passes through it to reach the absorbing plate. The plate heats up and transfers the heat to the heat transfer fluid circulating in the tubes. Like any heated body, the absorber emits radiation (mainly infrared) which is reflected by the glass, creating the greenhouse effect. The insulation's function is to minimize thermal losses to the outside. Indeed, the majority of the absorbed energy should be transmitted to the fluid. [11]

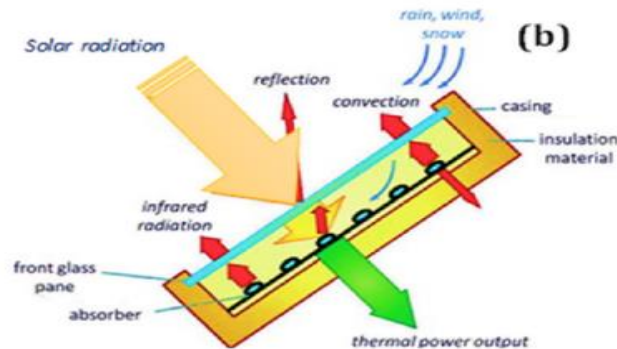


Figure I.7: heat transfer phenomena

Table I.2 shows some advantages and inconvenients of this type of collector

Table I.2:Advantages and disadvantages of glazed flat-plate collectors[12]

Advantages	Disadvantages
Long lifespan.	Suitable only for high temperatures.
Protection Against External Elements	The internal temperature can rise .
Energy efficiency.	quickly in the absence of heat transfer fluid circulation.

b. Unglazed Flat-Plate Collectors:

Unglazed solar collectors are characterized by an absorber without the glass covering. Since these collectors are not insulated, they are used for low-temperature applications where the requested temperature is lower than 30 °C. Unglazed solar collectors are typically made of black plastic, stabilized for resisting ultraviolet light. Since these collectors have no glazing, a high share of the solar radiation is absorbed. On the other hand, these collectors are not insulated, and a large part of the absorbed heat is lost, in particular under windy and not warm external conditions [11]. Therefore, the efficiency of these Less common than the glazed collector, also known as "carpet" collector [11] the unglazed flat-plate collector consists of an absorber without an enclosure or glazing, simplifying both its design and reducing manufacturing costs. However, this type of collector is highly dependent on ambient air temperature. While it performs well in the summer, it is highly sensitive to cold winds in winter due to the lack of a glass cover.

To achieve the same performance as a glazed flat-plate collector, it is generally necessary to install one and a half times more collector surface area. Consequently, the overall installation cost becomes comparable to that of a glazed collector. [12]

The common operating temperatures never exceed 30°C, which limits its use to:

- Heating swimming pools.
- Preheating hot water. [13]



Figure I.8: Unglazed Flat-Plate Collectors

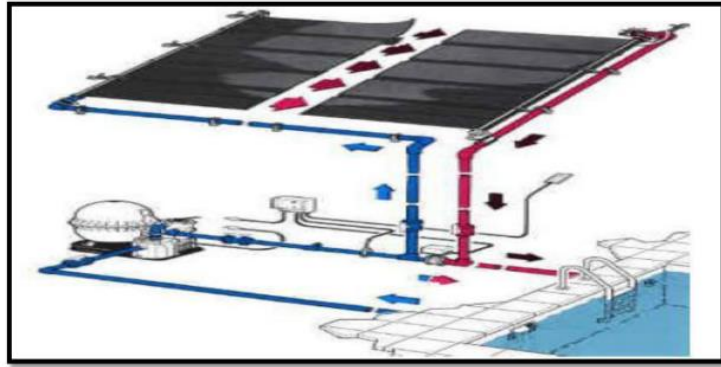


Figure I.9 Unglazed flat plate solar collector for used for pool heating

Table I.3:Advantages and disadvantages of unglazed flat-plate collectors. [12]

Advantages	Disadvantages
Lower cost.	Operates only at low temperatures.
High efficiency for temperatures <40°C.	Vulnerability to Environmental Damage
The absorber itself can serve as the building roof.	Limited Heat Retention

c. Vacuum Tube Collector

Conventional flat-plate solar collectors perform efficiently in sunny and warm conditions but suffer reduced effectiveness during cold, cloudy, or windy weather. [22]

The vacuum tube collector uses vacuum as a thermal insulation medium, which gives it high efficiency at high temperatures. It consists of:

- A series of vacuum glass tubes with a small diameter (up to about fifteen centimeters).
- An absorber inside the glass tubes.
- Copper tubes inside the glass tubes, through which a heat transfer fluid (water mixed with antifreeze) circulates. This fluid heats up as it flows through the tubes.

Thanks to the insulating properties of the vacuum, heat losses due to convection are greatly reduced. This allows the water to be heated to temperatures between 85°C and 100°C. Such high temperatures are required for industrial applications that use very hot water or steam. [13]



Figure I.10 : Vacuum tube solar collector

I.4.3.2. Concentrating Solar Collectors:

Concentrating solar collectors reflect and focus solar radiation directly onto the absorber, thereby increasing the intensity of the solar rays. Consequently, this type of collector can achieve significantly higher temperatures than traditional flat-plate collectors.

There are three main types of concentrating collectors :

- Cylindrical parabolic reflector.
- Parabolic reflector.
- Solar power tower [11].

a. Cylindrical parabolic reflector

Solar concentrators use reflective surfaces, such as parabolic or cylindrical-parabolic mirrors to concentrate solar rays either into a focal point or along a linear focus. These concentrators direct the solar radiation towards receivers (absorbers) located at the focal point or along the linear focus, where the concentrated solar heat is captured. It is important to note that these concentrators must track the movement of the sun to maximize the efficiency of heat capture.

[14]



Figure I.11:Cylindrical-Parabolic Collector

b. Parabolic reflector

A parabolic reflector system uses parabolic mirrors to concentrate solar radiation onto a receiver located at the focal point of the mirror. The receiver contains a fluid that, when exposed to sunlight, reaches temperatures between 750°C and 1,000°C. This very hot fluid is then used to produce electricity in a small engine attached to the receiver. Like the cylindrical-parabolic reflector system, the parabolic reflector also follows the sun's movement.[13]



Figure I.12 Parabolic reflector system

c. Solar power tower:

A solar power tower is a type of solar thermal system that uses a central tower surrounded by numerous heliostats (mirrors) to concentrate sunlight onto a receiver at the tower's top. This concentrated energy heats a fluid, such as molten salt, which stores the heat for generating steam to drive a turbine and produce electricity. This design enables high efficiency and energy storage, providing power even when the sun is not shining. Solar power towers are part of Concentrated Solar Power (CSP) technology.

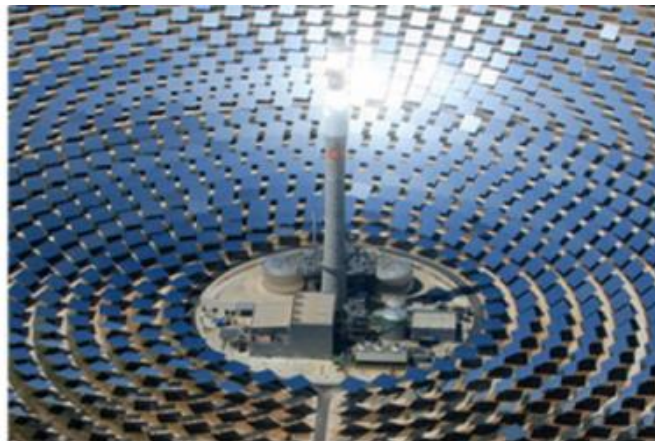


Figure I.13 solar power tower

I.5. Flat plate solar air collectors

I.5.1. Flat plate solar air collectors definition

The flat solar collector is a device designed to capture energy from solar radiation, convert it into thermal energy, and transfer it to a heat-transfer fluid. It operates based on two physical principles: the greenhouse effect and blackbody radiation. Flat-plate collectors can achieve temperatures ranging from 30°C to 90°C without requiring solar radiation concentration or sun tracking [15]

A collector consists of three main parts [14]:

- **Front section**

This is the transparent cover made of glass or plastic, which can be single, double, or triple-layered, its role is to Capture the maximum amount of incident radiation with minimal reflection or diffusion, transmit most of the received radiation and Prevent thermal losses through convection and radiation.

- **Absorbing section**

This is where thermal conversion takes place, and it must maximize radiation absorption, efficiently transfer heat to the fluid, and minimize external thermal losses.

- **Rear section**

This part typically consists of an insulating layer that reduces convection losses, thus slowing the cooling of the surface opposite to the solar radiation. The choice of material depends on resistance to high temperatures, long-term durability of thermal conductivity, and robustness against impacts, humidity, fire, and rain.

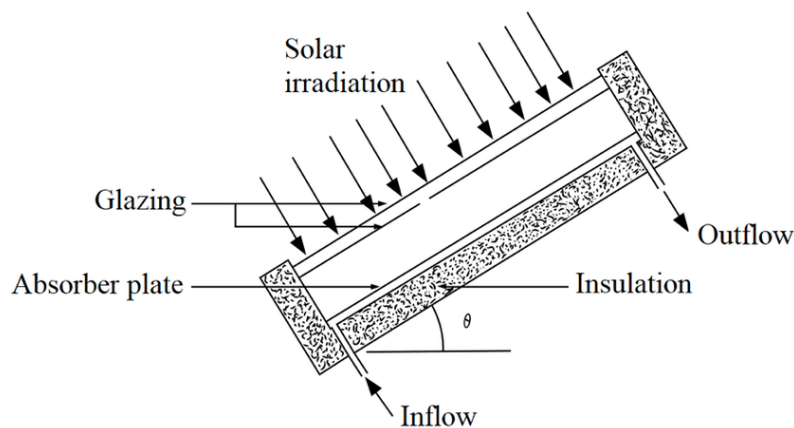


Figure I.14 : solar air heater

I.5.2. Role of each component

I.5.2.1. Transparent cover

The glazing creates a greenhouse effect, enabling temperatures to reach 70°C to 90°C and thereby improving efficiency. Solar collectors can feature one or multiple transparent covers.[16]

The cover serves as a mechanical protector for the absorber. Its main function is to reduce thermal losses to the outside [14]. The transparent cover plays several key roles in the solar collector system:

- **Protection:** It serves as a mechanical shield for the absorber, safeguarding it from environmental factors.
- **Thermal Insulation:** It helps reduce thermal losses to the outside by acting as a barrier to heat.
- **Convective exchange Control:** The space between the absorber and the cover (forming an immobile air gap) helps manage convective heat exchanges. The gap height typically ranges between 15 and 40 mm, helping retain heat within the system.
- **Radiative Exchange Management:** The cover allows solar radiation to pass through while blocking infrared radiation, ensuring efficient absorption and minimizing thermal losses.
- **Efficiency Improvement:** By creating a greenhouse effect, the transparent cover traps heat, boosting the system's overall efficiency and enabling the absorber to reach higher temperatures (over 70°C), while reducing cooling from wind exposure.

Most common transparent covers are made of simple or treated glass, allowing up to 95% of light to pass through. Synthetic materials are also available.

To further enhance the performance of solar collectors, manufacturers sometimes use two panes of glass:

- **The intermediate glass.**
- **The protective (or outer) glass:** This second pane has minimal impact on the greenhouse effect but primarily serves to improve the thermal insulation of the front face of the collector. The quality of this glass is just as important as that of the rear insulation.[17]

Glass remains the preferred material for this application, but it can undergo various treatments to enhance its properties. For instance, tempered glass offers excellent impact resistance, such as against hail. Additionally, adding metallic oxide layers creates selective glass that more effectively retains infrared radiation, thereby enhancing the greenhouse effect.[18]

Polycarbonates are plastic-derived materials consisting of very thin double or triple layers, interconnected by numerous partitions, forming honeycomb cavities. These cavities reduce the movement of trapped air within the structure, thereby minimizing thermal losses through convection at the front. When new, their solar radiation transmission coefficient is around 83% at normal incidence, decreasing slightly over time to approximately 79% after five years.

Polycarbonates offer several notable advantages: they exhibit excellent resistance to mechanical impacts and have a low density, which gives them low thermal inertia.[13]

I.5.2.2. The absorber

The absorber is the key component in the operation of a flat-plate solar collector. It consists of a surface with black body characteristics, serving three primary functions:

- Absorbing solar radiation,
- Converting this radiation into heat,
- Transferring this heat to the heat transfer fluid.

The selection of an absorber is based on several criteria:

- An absorption factor α as close to unity as possible,
- A low infrared emissivity ϵ .
- High thermal conductivity.
- Low thermal inertia.

The characteristics of various surface colors are given in the table I.4 [13]

The choice of materials and construction methods significantly impacts the overall quality of the collector. Due to their high thermal conductivity, copper, steel, and aluminum are the most commonly used materials [14]. Table I.4 shows some of the thermal characteristics of some absorber materials

The choice of material and the construction process have a significant influence on the quality of a collector. Due to their high thermal conductivities, copper, steel, and aluminum are the most commonly used materials.

The materials commonly used for absorbers include:

- **Copper:** recognized as the best absorber due to its excellent thermal properties, although it is the most expensive.
- **Aluminium:** valued for its lightness and good thermal conductivity. It also offers excellent corrosion resistance due to the formation of an alumina layer (Al_2O_3). To enhance its absorption capacity, the surface is coated with a thin layer of black paint.
- **Plastics:** These materials have the advantage of being lighter than metals and resistant to corrosion, making them particularly useful for specific applications.[13]

The characteristics of various materials used as absorbers are given in the table.I.4[13]

Table I.4 characteristics of materials used as absorbers

Material	Temperature (°C)	Thermal Conductivity $\lambda(\text{W/m}\cdot\text{K})$
Aluminum	100	0.49
	200	0.55
Copper	20	0.934
	100	0.908
	200	0.890
Magnesium	100	0.370

The absorber plays a crucial role in capturing solar radiation and converting it into thermal energy. Typically painted black, it absorbs most visible and ultraviolet radiation, along with a small amount of infrared radiation.

To maximize the absorption of solar energy, a flat surface must be strategically positioned, considering its tilt and orientation. Additionally, the surface layer should have the highest possible absorption coefficient.[13]

In solar heating applications, the goal is to achieve the best ratio of solar absorption factor to infrared emission factor. This ratio is known as selectivity.[19]

Table I.5:Absorption, reflectivity, and emissivity of different surface colors

Color	α	ρ	ϵ	α / ϵ
White Paint	0.2	0.8	0.91	0.22
Green Paint	0.5	0.5	0.9	0.56
Black Paint	0.96	0.04	0.9	1.0

To reduce radiation losses, absorbers are generally coated with a selective layer. Nickel and chrome are the main metals used for selective coatings in most collectors.

Table I.6 presents the most commonly used coating methods.

Table I.6 properties of some materials used as absorbers

Color	α	ϵ	α / ϵ	T_{max} (°C)
Black nickel	0.88-0.98	0.03-0.25	3.7-32	300
Graphitic films	0.876-0.92	0.025-0.061	14.4-36.8	250
Black copper	0.97-0.98	0.02	48.5-49	250
Black chrome	0.95-0.97	0.09-0.30	3.2-10.8	350-425

Key Characteristics:

The absorber must be a good thermal conductor while being lightweight to minimize thermal inertia. Some absorbers feature specially treated surfaces to trap solar rays more effectively. These surfaces must:

- Be thin to ensure efficient energy transfer.
- Maintain stability over time to retain their original properties.

The choice of materials and construction methods significantly impacts the overall quality of the collector. Due to their high thermal conductivity, copper, steel, and aluminum are the most commonly used materials [14].

Table I.6 shows some of the thermal characteristics of absorber materials.

Table I.7: Thermal characteristics of absorber materials

Material	Thermal Conductivity $\lambda(\text{W/m}\cdot^{\circ}\text{C})$	Specific heat capacity (Kcal/kg $^{\circ}\text{C}$)	Volumetric mass density (kg/m³)
Aluminum	230	0.214	2700
coper	380	0.094	8930
zinc	112	0.092	7130
steel	52	0.174	7900
inox	52	0.17	7900

I.5.2.3. Heat Transfer Fluids (Air)

The heat transfer fluid responsible for evacuating the heat stored by the absorber is atmospheric air. It transfers the recovered heat to the location where it is to be utilized.[19]

I.5.2.4. Insulation

To minimize the system's heat losses, it is essential to properly insulate its surfaces. At the front, an air gap typically acts as insulation, with an optimal thickness of 2 to 3 cm to reduce convective heat transfer. At the rear, one or more layers of insulation, such as glass wool, polystyrene, or polyurethane foam, are used.[18]

The use of air as the heat transfer fluid avoids the need for special heat transfer fluids (oil or glycol) able to withstand freezing

conditions.

- Corrosion is less of a concern.
- Leakage through joints and ducts is less of a concern.
- High-pressure protection is not required.
- The device is more compact and lightweight, less complicated and easy to install [20]

The insulation plays a crucial role in reducing heat losses and slowing down the cooling of the side opposite to solar radiation. A good insulator should have the following properties:

- Low density, to minimize thermal inertia.
- Low thermal conductivity.
- Low specific heat capacity.
- Thermal resistance suitable for the operating temperature range.[13]

To minimize heat losses in a system, it is crucial to insulate its surfaces. At the front, an air gap is typically used as insulation, but its thickness must be controlled to limit convective heat transfer. There are several types of insulators, classified into three main categories:

- **Mineral Insulators:**

- Glass wool.
- Vermiculite.

These materials have the advantage of withstanding temperatures above 250°C without degrading.

- **Plant-Based Insulators:**

- Wood [$k = 0.13-0.40 \text{ W/(m}\cdot\text{K)}$ between 0 and 200°C]
- Particleboard [$k = 0.05-0.10 \text{ W/(m}\cdot\text{K)}$]
- Sawdust [$k = 0.1 \text{ W/(m}\cdot\text{K)}$]
- Plant ash.

These insulators are abundant in tropical countries, making them particularly valuable because they not only tolerate high temperatures but are also virtually free in these regions.

- **Synthetic Organic Insulators:**

Table I.7 below provides an overview of the thermal properties of some insulating materials. [11]

Table I.8: Thermal properties of some insulating material

Materials	Thermal Conductivity at 25°C (W/m·K)	Maximum Temperature (°C)
Fiberglass	0.032	343
Polystyrene Foam	0.029-0.040	74
Polyurethane Foam	0.023	104
Phenolic Foam	0.033	135
Isocyanurate Foam	0.025	121

To minimize thermal losses at the periphery of the collector, one or more layers of insulation can be applied, which must withstand high temperatures without off-gassing. Otherwise, deposits may form on the inner surface of the cover. In addition to using insulation to reduce heat losses, the contact resistance between the plate, the insulation, and the casing can be increased by avoiding pressing these surfaces together. In cases of high roughness, an air film may form between the two contact surfaces, hindering efficient heat transfer through conduction. [14]

I.5.2.5. The casing:

The housing, or casing, forms the rear and lateral enclosure of the absorber and the thermal insulation of the collector.. It is made from selected materials such as sheet or profiled metals, reinforced plastics, or even plywood. Commonly used metals include galvanized steel, pre-painted galvanized steel, and aluminum alloys [3].

There are two types of casing structures :

- **Single casing:** Made from a single layer of material, it takes the form of a tray in which the insulation and absorber are installed.
- **Double casing:** Designed with a box structure, it provides greater rigidity and allows for better integration of the insulation.[14]

I.5.3. Parameters and Operating Characteristics of Solar Collectors

I.5.3.1. External parameters

External parameters include:

- **Solar Irradiation Parameter:** The energy illumination resulting from global solar radiation, influenced by the sun's position and the duration of sunlight.
- Ambient dry temperature.
- Wind speed over the collector.

I.5.3.2. Internal Parameters

Internal parameters consist of:

- **Position Parameters:** The tilt angle and orientation of the collector.
- **Collector Dimensions:** Thickness, length, width, and receiving surface area.
- **Cross-section of the heat transfer fluid passage.**

I.5.3.3. Operating parameters

Operating parameters are represented by:

- Inlet temperature of the fluid in the collector.
- Temperatures of different parts of the collector.
- Flow rate of the heat transfer fluid.[15]

In practice, depending on the specific solar energy application, the following guidelines apply:

- **Collector Placement:** Collectors should be positioned to avoid obstacles (shading effect) that block solar radiation from reaching the surface.
- **Orientation:** Mainly determined by the desired operation time during the day:
 - Morning operation: East-facing.
 - Afternoon operation: West-facing.
 - All-day operation: South-facing.
- **Inclination:** It varies based on the distiller's operational season:
 - Summer operation: Inclination angle = Latitude - 10°.
 - Winter operation: Inclination angle = Latitude + 20°.
 - Year-round operation: Inclination angle = Latitude + 10°.

Additionally, site-specific parameters should be considered, such as:

- **Geographical parameters:** Longitude, latitude, and solar altitude.
- **Meteorological parameters:** Cloud intermittency, percentage of diffuse radiation, wind, and ambient temperature.
- **Nature and socio-economic situation of the site:** Material selection, system automation level, infrastructure availability, and local workforce.[13]

I.5.4. Applications of Flat-Plate Solar air Collector

Solar energy can be directly converted into heat through thermal solar collectors, with various applications such as residential heating, crop drying (fodder, grains, fruits), and powering thermal engines. The main applications include:

I.5.4.1. Solar Drying:

Solar drying technology aligns with sustainable development principles, considering economic, sociocultural, and environmental factors to ensure the well-being of future generations. Solar drying is used either as a preservation method or as an essential step in the processing of certain products. It is widely employed in rural and industrial contexts, particularly in the agro-food sector. [21]. Air-based solar collectors are particularly effective for drying various agricultural products such as tea, coffee, fruits, beans, rice, spices, rubber, cocoa, and wood.

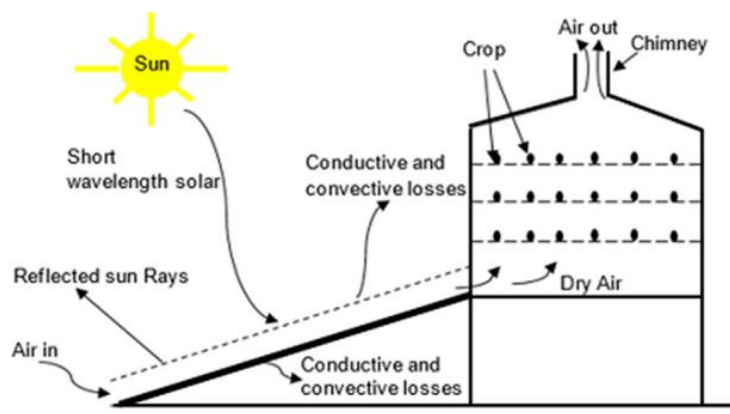


Figure I.15: Schematic view of the indirect type solar dryer

I.5.4.2. Heat Production for Residential Use

Used for heating and air conditioning of homes, the principle involves heating a fluid using a solar collector. The warmed air is then transported to various points of use by a fan, enabling the heating or cooling of residential spaces. [21]

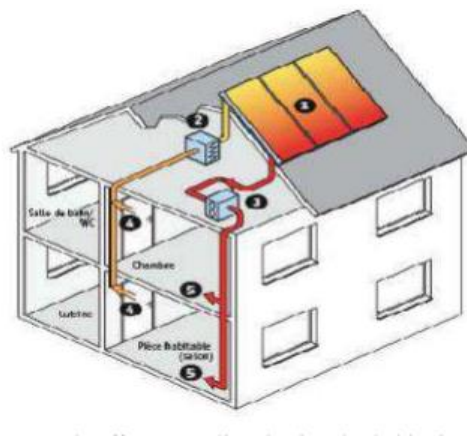


Figure I.16: Solar collector used for air conditioning

Solar energy can be directly harnessed for heating by exposing a material to solar radiation. This heat can be transferred to a suitable system to warm houses. One common method is the **Trombe-Michel Wall**:

- **The Trombe-Michel Wall:**

Named after Professor Félix Trombe, renowned for his work on solar furnaces, the Trombe-Michel wall is a system directly integrated into the structure of a house. A section of the exterior wall is replaced by double glazing, behind which a concrete wall is positioned inside the house. This system effectively captures and stores solar heat, redistributing it within the living space. [21]

The greenhouse effect principle is once again utilized in this system. The wall captures solar heat and warms the air between the concrete wall and the double glazing. Since hot air is less dense than cold air, it rises naturally, creating a circulation that heats the house. In this process, cold air inside the room is gradually replaced by the warm air from the space between the wall and the glazing.

The wall's thickness is designed to store part of the heat absorbed during the day and release it later, particularly at night. Heating occurs in two ways:

- **Directly through convection of warm air.**
- **Through slow infrared radiation:** the wall gradually transmits some of the accumulated heat to the room air via thermal radiation.[13]

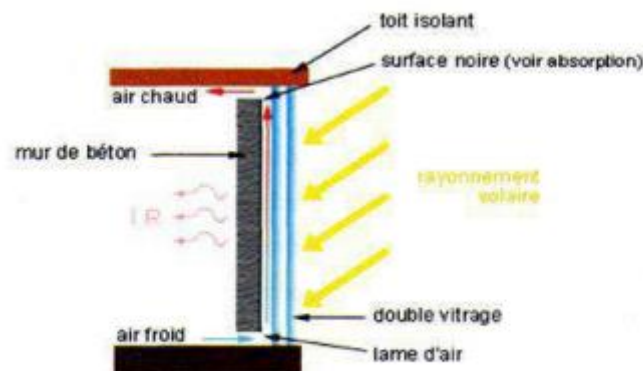


Figure I.17: The Trombe-Michel Wall

I.5.4.3. Mechanical Energy Production (Stirling Engine)

The Stirling engine, sometimes referred to as an external combustion engine or hot air engine, was invented in 1816. It has regained attention today due to its low pollution, high efficiency, and quiet operation.

The principle involves a sealed chamber where gas is heated on one side and cooled on the other. The resulting pressure variations drive a piston, which in turn operates a pump via a connecting rod.

I.6. conclusion

Solar technology holds significant potential in meeting the world's energy needs. However, its usage remains limited, primarily due to the high initial construction costs associated with solar systems. The performance of a solar collector largely depends on its ability to capture solar energy and efficiently transfer it to the heat-transfer fluid. Consequently, a study was conducted to assess the performance of solar collectors and analyze the parameters influencing their efficiency, aiming to promote better design and more effective utilization. [11]

This chapter introduced solar radiation and solar potential in Algeria, highlighting the country's favorable sunlight conditions. It also covered flat plate solar collectors, detailing their key components (absorber, glazing, insulation, casing) and their role in optimizing thermal conversion. This foundation enables a deeper study of collector performance and their adaptation to local climatic conditions.

Chapter II Literature review

II.1. introduction:

The production of thermal energy from solar power is currently one of the most promising techniques to meet global energy needs. Today, several million square meters of solar collectors and systems are installed worldwide, using the latest technologies. Most research focuses on improving the thermal performance of solar collectors by considering all parameters that influence their behavior, including design factors (geometric, thermophysical, and optical).

From various investigations, it was understood that heat transfer and collector efficiency were controlled by three factors, such as flow rate of air, airflow channel design, and absorber surface geometry

Investigations on different configurations of absorber:

II.2. Finned absorber plate:

The thermal performance of the SAC with and without fins was studied by **Daliran and Ajabshirchi [1]**. The maximum temperature and thermal efficiency by the experimental and theoretical study was 74.5 °C, 21% and 83 °C, 22%, respectively.

M.A. Karim et al [2] developed a mathematical modelling of counter flow v-groove solar air collector and simulation is carried out using MATLAB programme. The simulation results were verified with three distinguished research results and it was found that the simulation has the ability to predict the performance of the air collector accurately as proven by the comparison of experimental data with simulation. The difference between the predicted and experimental results is, at maximum, approximately 7% which is within the acceptable limit considering some uncertainties in the input parameter values to allow comparison. A parametric study was performed and it was found that solar radiation, inlet air temperature, flow rate and length have a significant effect on the efficiency of the air collector. Additionally, the results are compared with single flow V-groove collector.

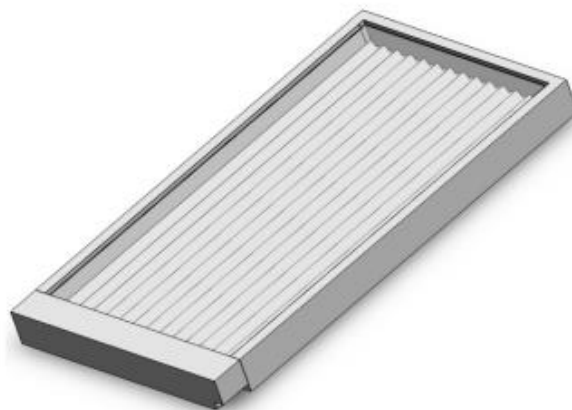


Figure II.1:Solar v-groove air collector

Rajesh Kumar, Prabha Chand [4] explore the thermal performance enhancement of solar air collectors through the integration of herringbone corrugated fins beneath the absorber plate within the fluid flow channel. The research employs a theoretical model based on energy balance equations, which is analysed using MATLAB simulations.

collector efficiency and air temperature rise are strongly influenced by mass flow rate. An increase in mass flow rate from 0.016 kg/s to 0.033 kg/s enhances collector efficiency by 18%, although it reduces the temperature rise by 15°C. For a fin pitch of 2.5 cm, thermohydraulic efficiency peaks at 68.96% at a mass flow rate of 0.05 kg/s, declining to 64.4% at 0.08 kg/s due to increased pressure drop. Reducing the fin pitch from 2.5 cm to 1 cm improves thermal efficiency from 66.85% to 71.40%, primarily due to an expanded heat transfer area. Furthermore, higher solar intensity consistently boosts thermal performance across all mass flow rates and fin pitches. However, thermal efficiency drops from 71.8% to 69.2% when the flow cross-section aspect ratio increases from 0.67 to 2, indicating the importance of optimizing structural design for maximum efficiency.

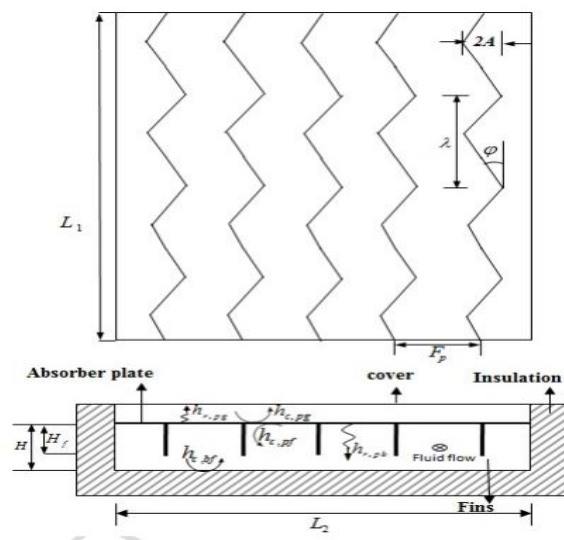


Figure II.2: Air heater with herringbone corrugated fins with geometrical description

Singh and Dhiman [5] analyzed the performance of a solar air heater (SAH) incorporating fins and baffles to enhance heat transfer. MATLAB was employed in the analysis to investigate the effects of parameters like mass flow rate, recycle ratio, fin thickness, number of fins, and baffle width on efficiency. They found that the heater with both fins and baffles achieved a thermal efficiency of 81%, outperforming the configuration with fins alone, which achieved a thermal efficiency of 79%. This study highlights the effectiveness of using baffles alongside fins in improving heat transfer by increasing turbulence and optimizing airflow within the heater.

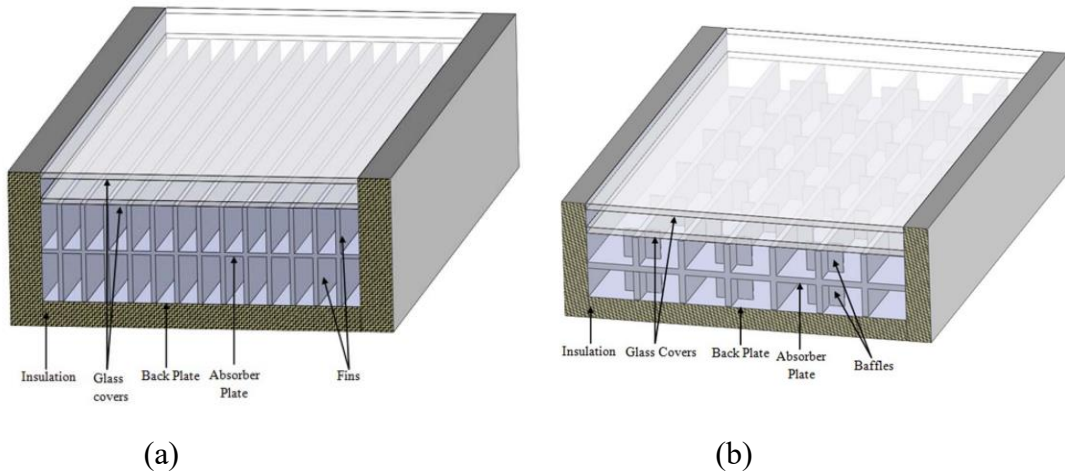


Figure II.3: Schematic diagram of double pass solar air heater with (a) fins and (b) fins with baffles.

Hassan and Abo-Elfadl [6] investigated the performance of the flat absorber plate, Pin-finned absorber plate, corrugated finned absorber plate and corrugated-perforated finned absorber plate were compared and concluded that the corrugated-perforated finned absorber plate has more benefits than the other. The maximum efficiency of 83% was achieved by using the corrugated-perforated finned absorber plate at the 66.7% of airflow in the upper port.



(a)



(b)



(c)



(d)

Figure II.4: Absorber plate configurations (a. flat plate, b. pin fins, c. corrugated fins, and d. corrugated-perforated fins)

The horizontal and vertical configurations of fins on absorber of SAC were investigated by **Maytham Ali Al-Neama & Istvan Farkas**[7] comparing the drying efficiency of solar dryer.

An experimental study was conducted to estimate the thermal efficiency of double-pass solar air collectors equipped with horizontal and vertical fins and integrated with a drying chamber. The setup consisted of two primary components: a solar collector and a dryer. The absorbers, made of copper, featured fins oriented horizontally and vertically. The results indicated that switching the fin orientation from vertical to horizontal increased the daily thermal efficiency by 10%. After 5 hours of drying 2 kg of apple slices, the final weights were 1.16 kg and 1.37 kg for the horizontal and vertical-finned collectors, respectively.



Figure II.5: (a) installation of solar drying system (b) Directions of fins on the absorbing surfaces of collectors (c) Design of drying chamber

Singh and Dhiman[8] demonstrated that incorporating baffles and fins in a solar air heater (SAH) resulted in greater heat transfer compared to a system equipped with fins alone. They concluded that the thermal efficiency achieved was 81% for the configuration with baffles and fins, compared to 79% for the heater with fins only.

II.3. Absorber with baffles and obstacles

Khanlari et al. [9] analyzed the thermal performance of a novel parallel-pass solar collector tested for drying applications featuring plus-shaped perforated baffles. The study compared three configurations: without baffles, with single baffles, and with double baffles. The baffles were designed in a plus-shaped, perforated structure to enhance thermal performance. Both

numerical and experimental analyses were conducted to evaluate the performance of these solar collectors. A drying chamber was integrated into the system, and celery root (*Apium graveolens L.*) was used as the test product. The average thermal efficiencies achieved were approximately 62%–66% for the collector without baffles, 65%–69% with single baffles, and 71%–75% with double baffles. The maximum deviation between experimental and numerical results was found to be 9.5%.

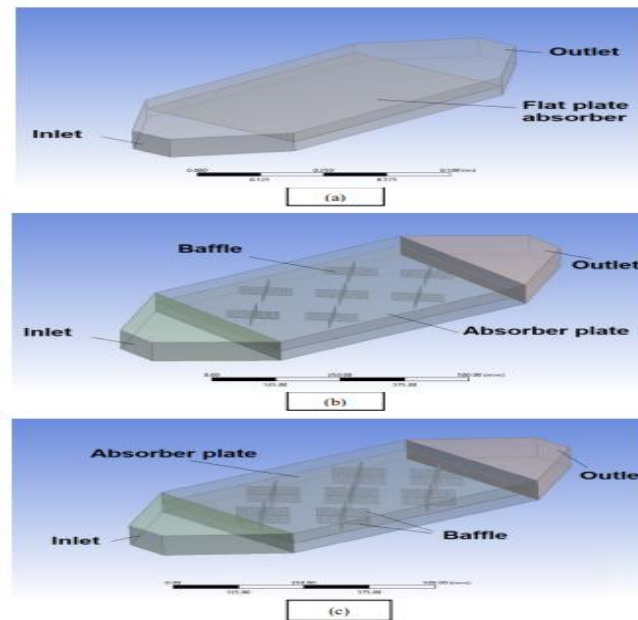


Figure II.6:Geometry of designed solar collectors; a) PPSC, b) PPSCB, c) PPSCDB.

Garcia et al. [10] conducted a study to explore enhancements in the thermal efficiency of solar flat plate collectors used for domestic water heating. The research specifically investigated the impact of adding convective barriers inside the air cavity between the absorber plate and the glass cover. These barriers reduce the air gap, potentially limiting heat loss and thereby improving the collector's thermal performance. The experimental setup included four solar collectors, each with different numbers of convective barriers (ranging from one to four), and their performance was compared to a reference collector without any barriers.

The results showed that there was no significant variation in solar radiation absorption since the maximum thermal efficiency remains unchanged. However, the barriers inclusion implies in changes in heat loss. The experimental data shown that changes in heat loss are $-2,2\%$, $-5,3\%$ and $2,9\%$ for two, three and four barriers, respectively. In this way, the convection barriers are able to reduce the heat loss in two cases, but increase the heat loss in one case. This result indicates that there is an optimal number of convective barriers for each solar collector design.

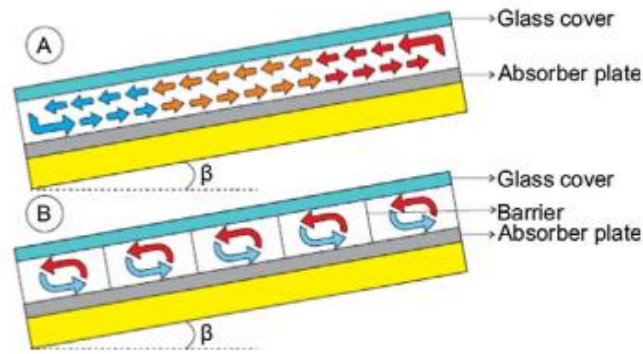


Figure II.7: Illustrative lateral view of the internal convection flow of the solar collector without barrier (A) and with Barrier (B).

II.4. Other competent improvements of flat plate solar air collector

Hassan et al [11] conducted an experimental study to assess the performance of a novel design of a solar air heater (SAH), referred to as the tubular solar air heater (TSAH). Unlike the conventional flat solar air heater (FSAH), the TSAH features adjacent tubes aligned with the airflow direction, replacing the flat absorber plate. To compare their thermal efficiency, two SAHs—identical in dimensions and materials except for their absorbers—were constructed and tested at varying airflow rates. This comparative analysis highlights the impact of absorber configuration on the overall performance of solar air heaters, contributing valuable insights into the optimization of solar thermal systems .

Results reveal that

- **Higher Efficiency and Output Power:** The TSAH demonstrates superior efficiency and output power compared to the FSAH. The TSAH also maintains a higher outlet air temperature and experiences lower top heat losses.
 - **Comparative Efficiency Gains:** The TSAH's efficiency significantly surpasses that of previous SAH designs. Specifically:
 - At an airflow rate of 0.025 kg/s, TSAH achieves a temperature increase of 13.2°C over the FSAH.
 - The average daily efficiency for TSAH reaches 83.6% at 0.075 kg/s, 76.3% at 0.05 kg/s, and 59.8% at 0.025 kg/s.
 - Compared to the FSAH, these efficiency levels represent increases of 132.6%, 58.6%, and 43.5%, respectively.
2. **Reduced Heat Loss:** The TSAH exhibits a 10% reduction in daily top heat loss compared to the FSAH, indicating better thermal retention.



Figure II.8: The experimental setup (front view)



Figure II.9: The absorber of the TSAH

C. Ramesh et al.[12] investigated the performance of solar absorber panels coated with black-chrome (BC) and nickel-cobalt (Ni-Co) coatings. The study also incorporated the use of reflectors to enhance solar radiation absorption. The experiment focused on the effects of three process variables—flow rate, collector angle, and reflector angle—on the thermal efficiency of the solar panel. The thermal efficiency was the primary response measured, with the goal of optimizing these factors to improve the overall performance of the solar thermal system.

The study demonstrates that the black-chrome (BC) coated panel significantly outperforms the nickel-cobalt (Ni-Co) coated panel in terms of thermal efficiency. The BC panel has an absorptance of 0.91 and a low emittance of 0.16, whereas the Ni-Co panel, despite its higher absorptance of 0.92, has a considerably higher emittance of 0.34. This increased emittance in the Ni-Co panel leads to greater energy losses, resulting in lower overall thermal efficiency.

On average, the BC panel achieves an efficiency of 58.67%, compared to 50.19% for the Ni-Co panel. The maximum efficiency for the BC panel is 89.3%, observed at a flow rate of 1.28 l/min, with a collector angle of 43.89° and a reflector angle of 44.92°. In comparison, the Ni-Co panel reaches a maximum efficiency of 79.2% at a flow rate of 1.32 l/min, a collector angle of 46.91°, and a reflector angle of 42.34°.

Overall, the BC panel demonstrates a 10.01% higher maximum efficiency, highlighting its superior performance and suitability for enhancing solar thermal systems.

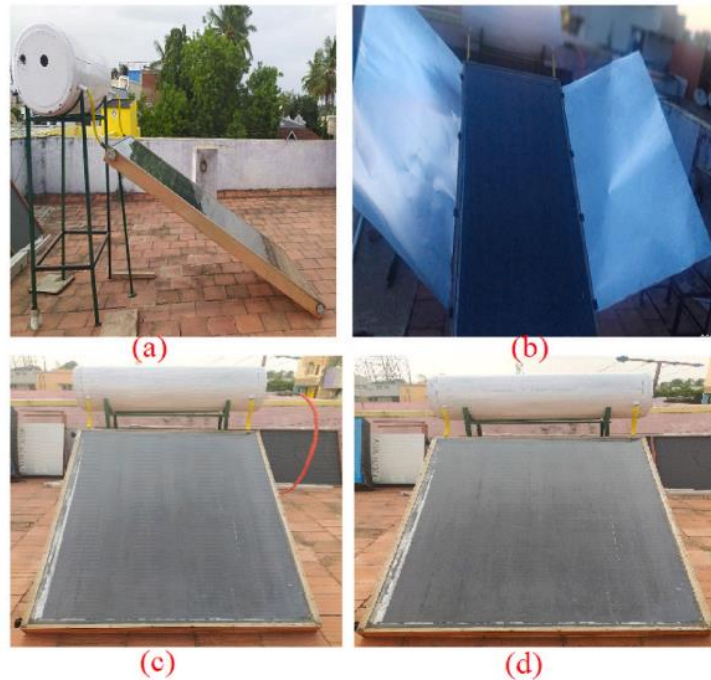


Figure II.10: .Experimental Setup (a) flat plate collector - with 45° inclination, (b) flat plate collector with reflectors, (c) flat plate collector with Black Chrome coating, (d) flat plate collector with nickel cobalt coating

Singh and Singh [13] developed a numerical model to examine the impact of various curvature angles on the thermal performance of curved solar air heaters (SAHs). The study revealed that the maximum outlet temperature was initially achieved at a curvature angle of 30°, but after reaching steady-state conditions, the highest temperature was attained with a curvature angle of 25°. Additionally, the results indicated that in the leeward position, curved SAHs with tilt angles ranging from 0° to 30° experienced minimal heat loss.



Figure II.11: Experimental set up

II.5. Thermal insulation:

Thermal insulation plays a crucial role in determining the thermal efficiency of a solar collector. In flat plate solar collectors, insulation serves to reduce heat loss through the rear of the collector after solar energy has been absorbed and stored. To ensure optimal performance, the insulation must effectively limit heat dissipation, even under standard operating temperatures.[16]

The impact of different insulation materials on thermal efficiency was analyzed by **Nadir N et al [14]**. This paper introduces a solar air heater that utilizes date palm wood, a widely available vegetable-based insulating material in tropical and Saharan regions, specifically designed for drying applications. The study emphasizes the comparative thermal performance of this collector against another with identical design and fabrication, operating under the same conditions but using glass wool as insulation including fiber in solid and powdered forms, petiole in piece and powdered forms, and combinations of petiole with gypsum as well as fibers with gypsum. Among these, the combination of petiole and gypsum demonstrated superior performance, achieving a 37% higher thermal efficiency compared to the collector insulated with glass wool. The average outlet air temperature of the collector insulated with glass wool was 7% lower than that of the collector insulated with a petiole and gypsum combination. This indicates that date palm wood serves as an effective and safe material for developing high-performance insulation.



Figure II.12: Photo of the solar air collector

II.6. Thermal energy storage:

We need solar energy with long-term availability, which is not possible when sunlight is not available, and it can be solved using TES. Thermal energy can be stored in the form of sensible heat, latent heat, and thermochemical energy.

Moradi et al. [15] conducted an optimization of solar air heaters (SAH) incorporating paraffin as a phase change material (PCM). The optimal results were achieved with a mass flow rate of 0.018 kg/s and a PCM thickness of 4 cm. Under these conditions, the temperature difference between the inlet and outlet was 4.5 °C. The optimal thermal conductivity and energy efficiency values were 1 W/m·K and 37%, respectively.

Vijayan et al. [16] investigated a solar dryer utilizing sensible heat storage (SHS) materials under varying air mass flow rates for drying bitter gourd slices. The system featured a black-coated, galvanized iron corrugated absorber sheet as the absorber plate, with pebbles serving as the SHS material at a height of 60 mm. The primary aim of the study was to examine the impact of air mass flow rate on the exergetic efficiency of the solar drying system. The findings revealed that the mass of bitter gourd slices was reduced from 4000 g to 723 g within 7 hours at an air mass flow rate of 0.0636 kg/s. Additionally, the average exergy efficiency ranged from 28.74% to 40.67% as the air mass flow rate varied between 0.0141 kg/s and 0.0872 kg/s.

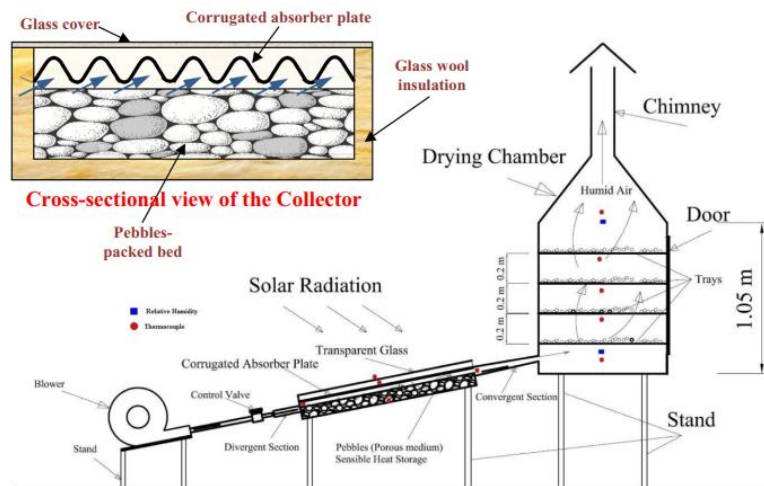


Figure II.13: solar dryer with heat storage

. Investigations and developments on hybrid photovoltaic/thermal solar air collector

The need for electrical energy requirement of SAC, space requirement of SAC and PV system, and the lower electrical efficiency PV panels brought the thought of combining these two systems to develop a hybrid PV/T solar air heating system

ElGamal and al aimed [17] to develop an integrated solar-tracking system to maximize the efficiency of solar heaters made from recyclable aluminum cans (RAC). The focus of their study was to enhance the drying process of apple slices using this innovative system. The results revealed that the thermal efficiency of the solar air heater incorporated with a tracking unit was significantly improved by about 45% compared with the conventional fixed heaters at all tested air flow rates. The highest thermal efficiency of 87.1% of the solar air heater equipped with a tracking unit was achieved at the highest air flow rate of $44 \text{ m}^3 \text{ h}^{-1}$. The highest moisture diffusivity (D_{eff}) at the high levels of drying air temperature and flow rate and the highest value of D_{eff} ($5.43 \times 10^{-10} \text{ m}^2 \text{ s}^{-1}$) was obtained in the dryer with a tracking system at the highest air flow rate of $44 \text{ m}^3 \text{ h}^{-1}$. The drying rate of apple slices under such a tracking module was considerably higher than that of either the traditional fixed system or the ambient sun drying.

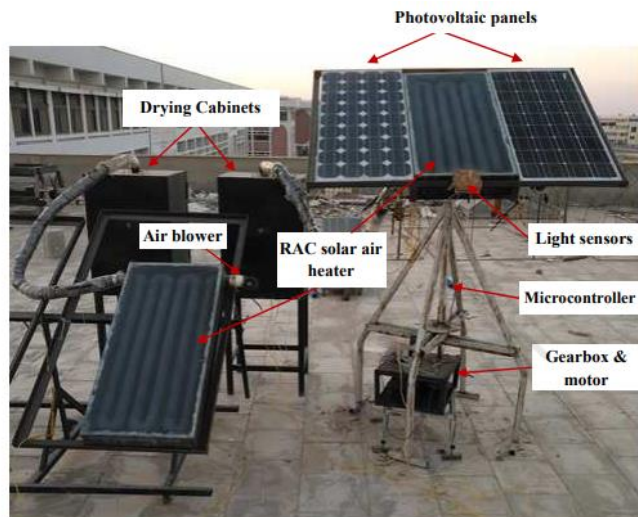


Figure II.14: Solar air heater integrated with drying cabinets

Chapter III

**Physical model ,mathematical
formulation and numerical solution.**

III.1. Introduction

This study explores the harnessing of solar energy through thermal methods, focusing on the production of heated air using a solar air collector.

In this chapter, we will present the details of a numerical procedure for a forced convection solar air heater, exposing the different steps to follow, starting from the energy balance equation to the numerical and graphical results with MATLAB. First, we will define the type of flat plate solar air collector used, outlining its operating. Subsequently, we will examine the various stages involved in the mathematical modelling of a double-pass solar air collector and its associated components. The objective is to develop a set of mathematical equations that will be solved using a numerical method.

III.2. Description of The flat-plate solar collector

The flat-plate solar collector measuring 1.2×0.6 m with a double pass is designed in two distinct parts. The upper part, exposed to sunlight, is protected by a standard transparent glazing with a thickness of 5 mm. Its purpose is to create a greenhouse effect inside the collector. A matte black flat-shaped absorber separates the lower part from the upper part. Its function is to capture as much radiation as possible during the day and convert it into thermal energy through the greenhouse effect, which is used to heat the circulating air. The lower part receives air through an opening (1st pass), then it flows beneath the absorber and is redirected to the upper part to achieve maximum heating. . Forced convection is achieved using a fan that draws the outside air and pushes it into the collector. The physical model of the considered solar collector is presented in Fig III.1

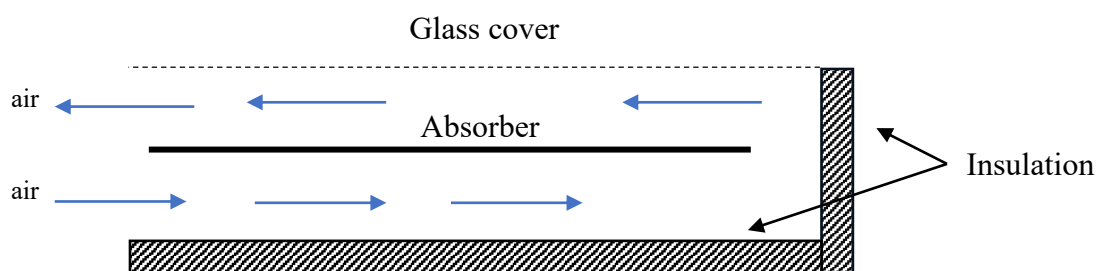


Figure III.1:Schematic Diagram of the Flat-Plate Solar Air Collector.

The solar collector was experimentally built in the ETAP laboratory to supply a drying chamber, figure III.2 represents two pictures showing a real view of the collector.



(A)



(B)

Figure III.2:(A) front picture of a solar air collector, (B) side picture of solar air collector.

The geometric parameters of the flat-plate solar collector used in our study are presented in the table III.1.

Table III.1: geometrical parameters of the collector

NUMERICAL PARAMETERS		
Parameters	Colonne1	Colonne2
Parameters	Values	Unit
Width of the collector	0.6	m
Length of the collector	1.2	m
Height of the first passage	0.12	m
Height of the second passage	0.06	m

III.3. Mathematical modelling:

The mathematical modelling of heat transfer is derived from energy balance equations that reflect the principle of energy conservation.

The assumptions imposed in our model are as follows:

- The sky is considered as a black body with an equivalent temperature calculated.
- The temperature of the various components varies only along the direction of air flow (x-direction).
- Thermal losses and air leakage to or from the collector are negligible;
- The airflow rate is steady;
- The thermophysical properties of the materials are assumed to vary with ambient temperature.
- The transparent glass cover is opaque to infrared radiation.
- The air between the glass and the absorber is assumed to be transparent.

For our study, the thermal exchanges occurring at the level of the flat plate collector, which take place through two well-known modes of heat transfer: **convective and radiative**, are schematized in the figure **Figure III.3** :

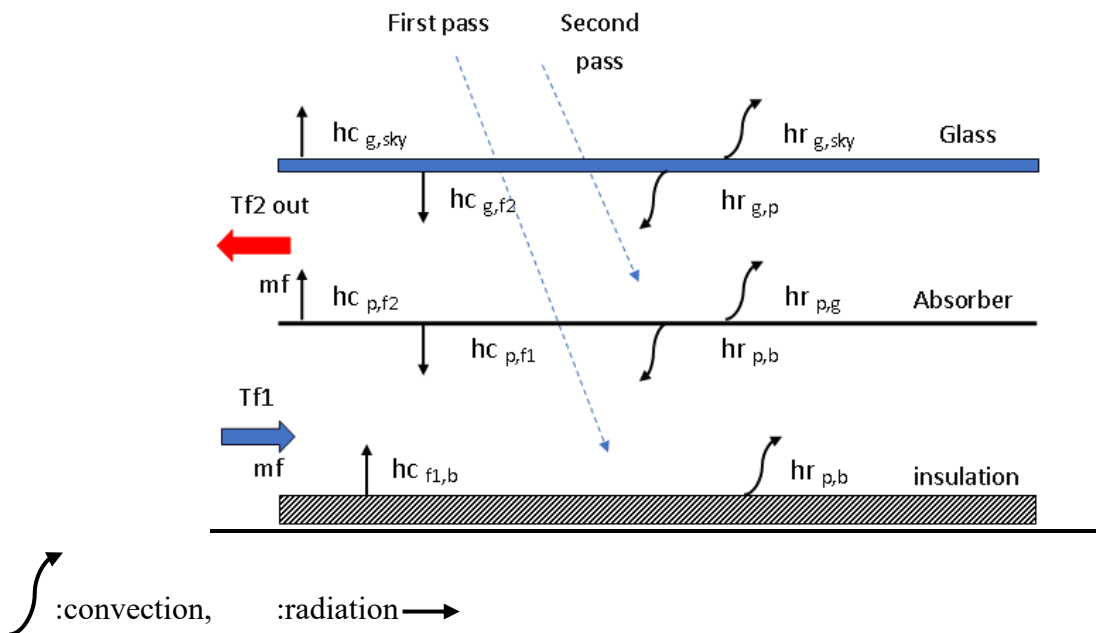


Figure III.3: Thermal exchanges between the components of a flat plate solar air collector."

III.4. Evaluation of Thermal Coefficients and Dimensionless Numbers

III.4.1. Thermal transfer by convection

Heat exchange by convection can occur:

- Outside the collector, between the collector and the surrounding ambient environment (exchanges due to wind).
- Inside the collector, between the absorber and the air confined in the glass-absorber space (or between this air and the glass or between insulation and air).

III.4.1.1. Thermal exchange by convection due to wind:

The coefficient for the external airflow over the glass cover is determined using the equation expressed as follows.[hassan ali]

$$h_w = 5.67 + (3.86 V_w) \quad \text{III.1}$$

with:

V_w : Velocity of the Wind

III.4.1.2. Thermal exchange by convection between surfaces and airflow through the collector

The forced convection heat transfer coefficient between the glass and the absorber is expressed as a function of the following dimensionless numbers:

Regarding forced convection, the average heat transfer coefficient is calculated as follows:

$$h_c = \frac{Nu K}{D_h} \quad \text{III.2}$$

where D_h is the hydraulic diameter of the duct. In the case of non-circular cross-sections, D_h is given by:

$$D_h = \frac{4A}{P} \quad \text{III.3}$$

Where A is Cross-sectional Area and P is wetted perimeter, The formula provides a practical method to characterize non-circular ducts by equating them to a circular duct of an equivalent diameter. This simplification facilitates the analysis of fluid flow and heat transfer in various engineering applications. However, careful consideration of geometry, flow conditions, and assumptions is crucial to ensure accurate results.

The Reynolds number is defined as:

$$Re = \frac{\rho v D_h}{\mu} \quad \text{III.4}$$

This expression evaluates the ratio of inertial forces to viscous forces for the fluid flow a higher Reynolds number indicates that inertial forces dominate, leading to a more turbulent flow.

Where v is the velocity are calculated with this equation:

$$v = \frac{m_f}{\rho A} \quad \text{III.5}$$

Where m_f is the masse flow rate of fluid and ρ is the **density and A is the section**

The formula:

$$Nu = 0,023 Re^{4/5} Pr^{1/3} \quad \text{III.6}$$

Where Pr is the Prandtl number

This equation determines the **Nusselt number**, a dimensionless parameter that quantifies the enhancement of heat transfer by convection relative to pure conduction in a fluid flow. It is derived from the **Dittus-Boelter correlation**, a widely used empirical relationship in heat transfer analysis for turbulent flow in circular and non-circular tubes or channels.

III.4.2. Thermal transfer by radiation

Thermal exchange by radiation occurs between:

- The outer surface of the collector's glass and the sky.
- Between the surfaces in the inlet of the collector .

III.4.2.1. Thermal exchange by radiation between the glass and the sky

The glass of the solar collector exchanges energy by thermal radiation with the sky. The radiative exchange coefficient Is given by:

$$h_{r,g,sky} = \sigma \epsilon_g (T_g + T_{sky}) (T_g^2 + T_{sky}^2) \quad \text{III.7}$$

where:

ϵ_g is Emissivity of the glass.

T_{sky} is the equivalent sky temperature is given by the SWINBANK relation.

$$T_{sky} = 0,0552 T_{amb}^{3/2} \quad \text{III.8}$$

T_{amb} is the ambient temperature .

III.4.2.2. Thermal exchange by radiation between each pair of interior surfaces of the collector:

The radiative coefficients depend on the temperatures of the surfaces on both sides.

$$h_r = \frac{\sigma(T_1^2 + T_2^2)(T_1 + T_2)}{\left(\frac{1}{\epsilon_1} + \frac{1}{\epsilon_2} - 1\right)} \quad \text{III.9}$$

III.5. Overall thermal balance of a flat plate air collector in transient state:

The purpose of the modelling is to predict the temperatures of each layer of the collector (glass, absorber, heat transfer fluid, and insulation). To achieve this, the principle of energy conservation is applied to each component of the system. This principle is expressed through an energy balance equation, which can be written as follows:

$$\left\{ \begin{array}{l} \text{The variation in internal} \\ \text{energy (accumulation term)} \end{array} \right\} = \left\{ \begin{array}{l} \text{the energy received by the} \\ \text{element (incoming)} \end{array} \right\} - \left\{ \begin{array}{l} \text{the energy lost by the} \\ \text{element (outgoing)} \end{array} \right\}$$

$$E_{\text{stored}} = E_{\text{in}} - E_{\text{out}}$$

Alternatively, in mathematical form, considering an arbitrary section of the system at time t , the energy balance at node 'i' is written as:

$$M_i C_i \frac{dT_i}{dt} = \sum_{in} Q - \sum_{out} Q \quad \text{III.10}$$

Where M_i and C_i represent the mass and specific heat capacity of the component and:

$M_i C_i \frac{dT_i}{dt}$ it is the thermal energy stored by the component.

$\sum_{in} Q$ it is the sum of the energies absorbed by the system through three modes of heat transfer (conduction, convection, and radiation).

$\sum_{out} Q$ is the sum of the energies lost by the system through the three modes of heat transfer (conduction, convection, and radiation).

III.5.1. Analytical expressions for energy balance

The thermal balance equations for the different components of the collector are expressed per unit area of the collector.

III.5.1.1. For the insulation (bottom)

$$m_b \cdot C_{pb} \cdot \frac{dT_b}{dt} = hc_{f1b} (T_{f1} - T_b) + hr_{pb} (T_p - T_b) + U_a \cdot (T_{amb} - T_b) \quad \text{III.11}$$

C_{pb} : specific heat of the insulation.

hc_{f1b} : convective heat transfer coefficient between the insulation and the working fluid.

hr_{pb} : radiative heat transfer coefficient between the insulation and absorber.

U_a : overall heat loss coefficient.

III.5.1.2. For first-pass air stream

$$hc_{f1b} (T_b - T_{f1}) A_b + hc_{f1p} (T_p - T_{f1}) A_p = m_f C_f \frac{dT_{f1}}{dt} \quad \text{III.12}$$

hc_{f1b} : convective heat transfer coefficient between the insulation (bottom) and the working fluid.

hc_{f1p} : convective heat transfer coefficient between the absorber and the working fluid.

III.5.1.3. For the absorber

$$\tau_g \cdot It \cdot \alpha_p = hc_{f1p}(T_p - T_{f1}) + hr_{gp}(T_p - T_g) + hc_{f2p}(T_p - T_{f2}) + hr_{pb}(T_p - T_b) + m_p \cdot C_{pp} \cdot \frac{dT_p}{dt} \quad \text{III.13}$$

hr_{gp} : radiative heat transfer coefficient between glass cover and absorber.

hr_{pb} : radiative heat transfer coefficient between absorber and isolation.

hc_{f1p} : convective heat transfer coefficient between absorber and working fluid1.

hc_{f2p} : convective heat transfer coefficient between absorber and working fluid2.

It : solar radiation.

τ_g : transmissivity of glass.

α_p : absorptivity of absorbent.

C_{pp} : Specific heat of absorber.

III.5.1.4. For second-pass air stream

$$hc_{f2g} \cdot (T_g - T_{f2}) A_g + hc_{f2p} (T_p - T_{f2}) A_p = m_f \cdot C_f \cdot \frac{dT_{f2}}{dx} \quad \text{III.14}$$

m_f : masse flow

C_f : Specific heat of fluid

III.5.1.5. For the glass cover

$$It \cdot \alpha_g = hc_{g,sky}(T_g - T_{sky}) + hr_{g,sky}(T_g - T_{sky}) + hc_{f2,g} (T_g - T_{f2}) + hr_{p,g}(T_g - T_p) + m_g C_{pg} \frac{dT_g}{dt} \quad \text{III.15}$$

m_g : mass of glass cover.

$hc_{g,sky}$: convective heat transfer coefficient between glass cover and sky.

$hr_{g,sky}$: radiative heat transfer coefficient between glass cover and sky.

$hr_{p,g}$: radiative heat transfer coefficient between glass cover and absorber.

C_{pg} : Specific heat of glass cover.

$hc_{f2,g}$: convective heat transfer coefficient between glass cover and fluid 2.

III.5.1.6. Global energy losses

Thermal losses are due to the temperature difference between the absorber and the surrounding environment. These losses manifest through three modes of heat transfer and are categorized into three types: losses towards the front, losses towards the rear, and lateral losses.

The following assumptions are made to simplify the determination of the loss coefficients:

- The solar power absorbed by the glazing is negligible.

- Lateral losses are small compared to the front and rear losses.

These assumptions help to focus on the primary heat loss directions (front and rear) and streamline the calculation of thermal losses, while neglecting smaller contributions such as lateral losses and glazing absorption.

The overall thermal loss coefficient towards the outside is the sum of the two previously determined coefficients:

$$U_{\text{total}} = U_{\text{front}} + U_{\text{rear}} \quad \text{III.16}$$

Where:

- U_{total} is the total thermal loss coefficient towards the outside.
- $U_{\text{front}} = U_a$ is the thermal loss coefficient towards the front.
- $U_{\text{rear}} = U_b$ is the thermal loss coefficient towards the rear.

This total loss coefficient accounts for all thermal losses through both the front and rear surfaces of the collector.

- **Expression of the thermal loss coefficients towards the front of the collector:**

The thermal losses towards the front of the collector are primarily due to radiation and convection from the glass cover and insulation surface to the environment. The loss coefficient can be expressed as a combination of these two modes of heat transfer.

$$U_{\text{front}} = \left(\frac{1}{h_{r_{g-sky}} + h_{r_{g-sol}} + h_{c_{g-amb}}} + \frac{e_v}{k_v} \right)^{-1} \quad \text{III.17}$$

- **Expression of the thermal loss coefficient towards the rear of the collector:**

This coefficient is generally less significant than the one for the front, as the collector is well-insulated at the rear. The expression for evaluating this coefficient is given by:

$$U_{\text{rear}} = \left(\frac{e_{\text{insulation}}}{k_{\text{insulation}}} + \frac{e_{\text{plywood}}}{k_{\text{plywood}}} \right)^{-1} \quad \text{III.18}$$

III.5.2. boundary conditions

In the first channel, the air temperature at the entrance of the solar collector is equal to the ambient temperature. At the right end, the temperature is assumed to be steady.

$$T_{f1}(x = 0) = T_a \quad \frac{\partial T_{f1}}{\partial x} \Big|_{\{x=L\}} = 0 \quad \text{III.19}$$

In the second channel, the air temperature is assumed to be steady at the exit. At the right end, the air temperature is assumed to be continuous.

$$\frac{\partial T_{f2}}{\partial x} \Big|_{\{x=0\}} = 0 \quad T_{f2}(x = L) = T_{f1}(x = L) \quad \text{III.20}$$

III.5.3. thermal efficiency

The thermal efficiency of the solar collector, defined as the ratio between the useful energy recovered and the total incident radiation, is given by:

$$\eta = \frac{m_f \cdot C_f (T_{f2out} - T_{amb})}{I_t A_s} \quad \text{III.21}$$

where I_t is the solar intensity (W/m^2) and A_s is the section)

III.5.4. The physical properties

The physical properties of air are assumed to vary with temperature:

- Specific heat of fluid:

$$C_f = 1005 + 0.1 (T_{amb} - 298) \quad \text{III.22}$$

- Density:

$$\rho = 1.225 \left(\frac{94981}{101325} \right) \left(\frac{288.15}{T_{amb}} \right) \quad \text{III.23}$$

The number 94981 Pa represents the local pressure in TLEMEN (Altitude 750m, Latitude 35° 28'N and Longitude 17° 1') and 101325 Pa is the atmosphere pressure and 288.15 K is the standard temperature.

- Thermal conductivity:

$$K = 2.646 \times 10^{-3} + (7.422 \times 10^{-5}) T_{amb} - (1.679 \times 10^{-8}) T_{amb}^2 \quad \text{III.24}$$

- Viscosity:

$$\mu = 1.460 \times 10^{-5} \frac{\left(\frac{T_{amb}}{288.15} \right)^{1.5} (288.15 + 110.4)}{T_{amb} + 110.4} \quad \text{III.25}$$

110.4 is a constant related to the temperature dependence of viscosity and 1.460×10^{-5} is the reference dynamic viscosity of air at a standard temperature 288.15K (15°C) in units of $kg \cdot m^{-1} \cdot s^{-1}$

III.6. Numerical Modelling

A thermal system is described by temperatures, temperature gradients, heat transfer coefficients, and so on. The equations used to represent such dynamic behaviours include unknown quantities that correspond to the desired functions and their derivatives, known as differential equations. There are several numerical approximation methods available for solving these equations:

1. The finite difference method (FDM).
2. The finite volume method (FVM).
3. The finite element method (FEM).

These methods offer different approaches for discretizing the equations and approximating solutions, each with its own strengths depending on the specific problem being addressed.

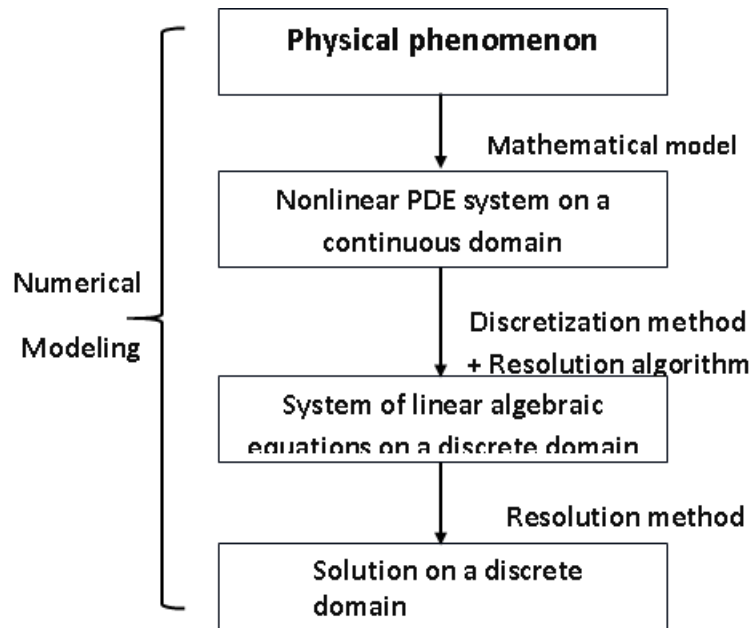


Figure III.4: The Principle of Numerical Calculation.

in this study, we used the finite difference method.

III.6.1. Principle of the Finite Difference Method (FDM)

The method involves approximating the derivatives of the physical equations using Taylor series expansions, and it directly follows from the definition of the derivative. This method is based on the assumption that when the spatial domain is divided into a finite number of intervals and the temporal domain into a finite number of time steps, the system can be discretized and approximated.

Advantages:

- Great simplicity in formulation.
- Low computational cost.

Inconvenances :

- Limited geometry for the computational domains.
- Difficulties in handling boundary conditions related to derivatives.

Here are some formulas for approximating the first derivative:

Table III.2:Numerical Schemes of Partial Derivative

Partial derivative	descritization	type
$\frac{\partial U(x_i, t^k)}{\partial x}$	$\frac{U^k_{i+1} - U^k_i}{\Delta x}$	Front
$\frac{\partial U(x_i, t^k)}{\partial x}$	$\frac{U^k_i - U^k_{i-1}}{\Delta x}$	rear
$\frac{\partial U(x_i, t^k)}{\partial x}$	$\frac{U^k_{i+1} - U^k_i}{2\Delta x}$	Centered

To solve the system of equations (S) in this model, we selected the explicit finite difference method for numerical resolution, resulting in:

```

for i=2:n-1
Tb(i,j+1) = Tb(i,j) + (dt*Ab / (Mb * Cpb)) * ((Tb(i,j)*(-hflb(j)-Ua)+(hflb(j)*Tf1(i,j)+(Ua*tamb(j))));

Tf1(i,j+1)=((dx/(mf*cp(j)))*((-Tf1(i,j)*hflb(j)*Ab)+(-Tf1(i,j)*hflp(j)*Ap)+...
(Tb(i,j)*Ab*hflb(j)+(Tp(i,j)*Ap*hflp(j))))+Tf1(i-1,j);

Tp(i,j+1) = Tp(i,j) + ((dt*Ap/(Mp*Cpp))*((It2(j)*alphaP*Tov)+(hflp(j)*Tf1(i,j)+(hrvp(i,j)*Tv(i,j)+(hf2p(j)*Tf2(i,j)+(hrpb(i,j)*Tb(i,j))...
+(-hflp(j)+hf2p(j)+hrpb(i,j)+hrvp(i,j))*Tp(i,j))));

Tf2(i,j+1) = ((dx/(mf*cp(j)))*((-Tf2(i,j)*hf2v(j)*Av)+(-Tf2(i,j)*hf2p(j)*Ap)+(Tv(i,j)*Av*hf2v(j)+(Tp(i,j)*Ap*hf2p(j))))+Tf2(i-1,j);

Tv(i,j+1) = Tv(i,j) + ((dt*Av/(Mv*Cpv))*((It2(j)*alphaV)+(hvf2(j)*Tf2(i,j)+(hrvp(i,j)*Tp(i,j)+(hrva(i,j)+hva(j))*Tsky(j))...
-(hvf2(j)+hrvp(i,j)+hrva(i,j)+hva(j))*Tv(i,j)));

end

```

For the simulation, we developed a program using MATLAB .

The heat transfer characteristics of solar air heaters are governed by Eqs. (11)–(15). To facilitate the analysis, the solar air heater is divided into multiple sections, as illustrated in Figure III.6.1 with calculations performed incrementally along its length. Solving the model requires determining the convective heat transfer coefficients for two key regions: the air flowing over the outer surface of the top glass cover and the air circulating within the system. Figure III.6 shows the flowchart of the steps used in the numerical calculation.

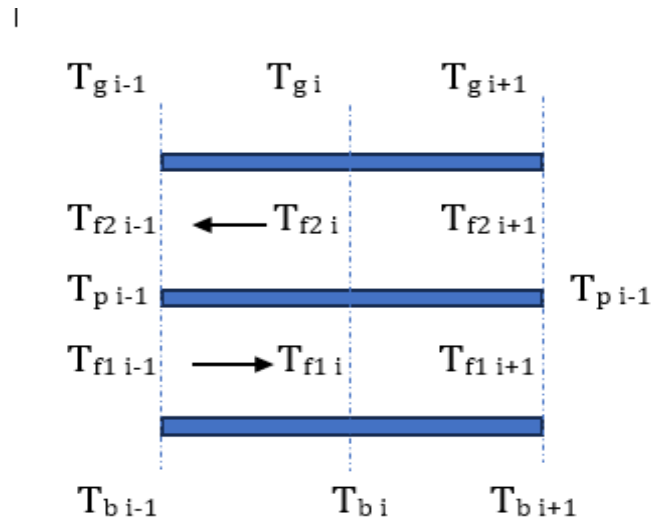


Figure III.5: Meshing for Numerical Calculation

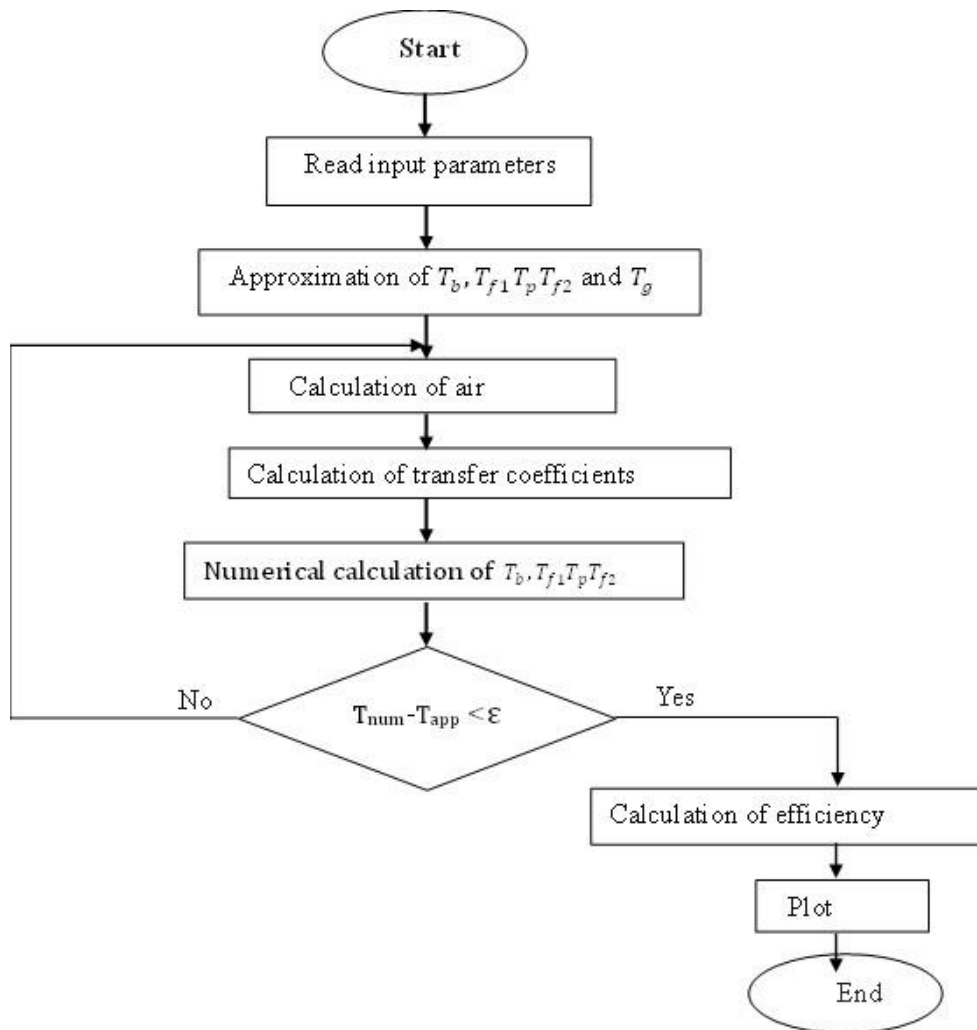


Figure III.6: Flowchart of the Numerical Calculation

III.6.2. The General Algorithm:

The algorithm for calculating the performance of the air solar collector consists of the following steps:

Step 1: Introduce data that do not depend on the "unknown" temperatures. This includes :

- The dimensions of the flat-plate air collector (length, width, thickness, tilt angle, etc.).
- The physical properties of the components of the collector that exchange heat by radiation (emissivity's, absorptivity's, transmissivities).
- The thermal conductivities of each element of the collector.
- Meteorological data, such as global radiation, ambient temperature, and wind speed.

Step 2: All data that depend on temperature are evaluated by the program according to the thermal balance equations. An iterative loop is initiated to calculate the different temperatures.

The tasks include:

- **Calculation of the properties of the heat transfer fluid (air)**
- **Calculation of transfer coefficients**, such as:
 - Radiative transfer coefficients
 - Conductive transfer coefficients
 - Convective transfer coefficients
- **Calculation of thermal loss coefficients:**
 - Losses at the front. (eq III.17)
 - Losses at the rear. (eq III.18)
 - Total losses

Step3: Calculate the efficiency using equation (III.21).

The temperatures (T_g T_{f1} T_{f2} T_p T_b) are obtained by solving the energy balance equation.

Step 4: The expected results are displayed in the form of curves. The quantities visualized include:

- Temperatures
- Thermal efficiency

III.7. Analysis of diurnal variation of solar radiation on ambient temperature:

The hourly evolution of ambient air temperature and solar radiation is presented in Figure III.1. The climatic data for a day in september for the region of Tlemcen were selected. a period characterized by noticeable changes in solar radiation and ambient temperature throughout the day. These daily fluctuations, referred to as diurnal variations, are driven by the sun's position

in the sky, which directly impacts the amount of solar energy reaching the Earth's surface. This, in turn, influences the atmospheric temperature.

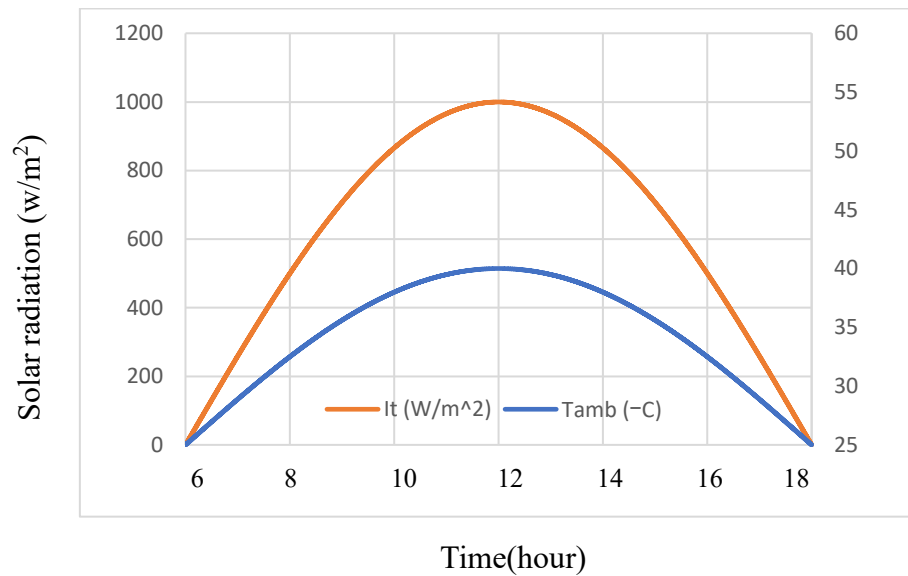


Figure III.7:Diurnal variation of average solar radiation on ambient temperature

The ambient temperature typically follows a predictable pattern during the day: it is lowest in the early morning, rises steadily to reach its peak in the early or mid-afternoon, and gradually decreases again during the evening and night. This temperature cycle closely aligns with the variations in solar radiation, which serves as the primary source of thermal energy. However, the connection between solar radiation and temperature is influenced by various additional factors.

- Cloud cover, which can reduce the intensity of solar radiation
- Atmospheric conditions, such as humidity and wind, that affect how heat is absorbed and distributed.
- Surface characteristics, such as glass, wood, black surfaces, which determine how energy is stored and released.

III.8. Conclusion

This chapter outlined the methodology and numerical approach employed to simulate the performance of the air solar collector. Using the finite difference method, we discretized the governing equations and employed an iterative process to solve for the system's temperatures and related thermal properties. The algorithm was carefully structured, starting with the introduction of physical parameters, followed by the calculation of heat transfer coefficients, thermal losses, and, ultimately, the system's efficiency. The results, including temperature profiles and thermal efficiency, were presented in graphical form, offering clear insights into the collector's performance under various conditions.

Chapter IV

Results and discussion

IV.1. Introduction:

This chapter presents the results obtained from the thermal simulations conducted on the solar collector, considering the physical and mathematical models introduced earlier. The simulations aimed to evaluate the impact of factors such as solar radiation fluctuations and air mass flow rate on the collector's thermal performance, offering insights into how each factor influences the system's energy efficiency. Furthermore, it will offer recommendations for optimizing the collector's performance under real-world operational conditions.

IV.2. Temperature evaluation in the solar collector

Figure IV.1 illustrates the temporal evolution of the temperatures of various components of the solar collector, including the inlet and outlet temperatures, as well as the temperatures of the absorber and glazing. These temperatures were recorded based on an ambient temperature ranging from 22°C to 35°C (September, 7th 2024), and these values may differ if a different month is considered.

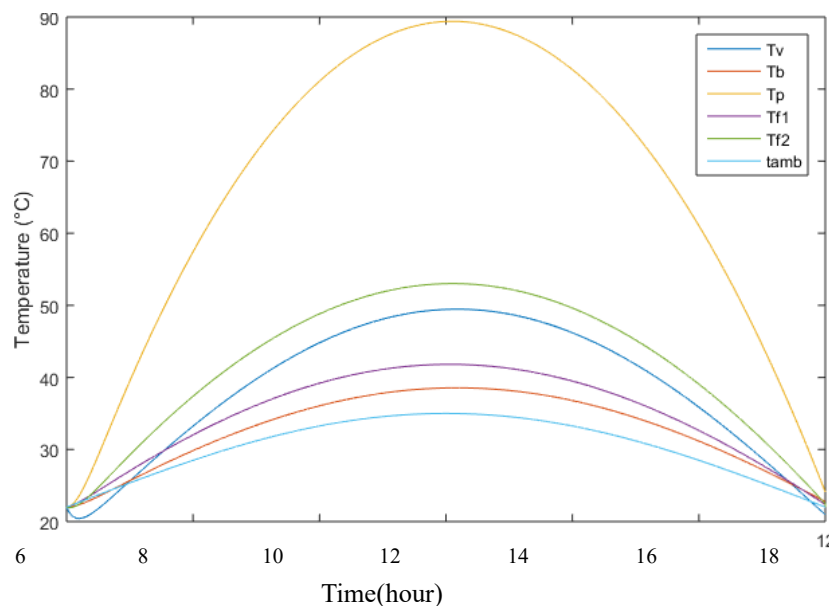


Figure IV.1:temporal evolution of the temperatures of various components of the solar collector

It is observed that the component temperatures increase throughout the morning, reaching a peak of 89.9°C for the absorber around 14:00 with intensity radiation of 850 (w/m²), followed by a decrease in the evening. The heating of the air inside the collector by the absorber results in a maximum temperature of 53°C at the outlet. The temperature of the glazing also increases over time reaching maximum of 48°C. This glazing plays a critical role in trapping infrared rays, which contribute significantly to the heating of the air circulating within the collector.

Where:

T_v : the glass cover temperature , T_b : the insulation temperature, T_p : the absorber plate temperature , T_{f1} : the first air stream fluid , T_{f2} : the second air stream fluid, T_{amb} : the ambient temperature .

IV.3. Spatial temperature evolution of air through the collector

In a double-pass solar collector, the air undergoes heating in two distinct stages. Initially, in the first pass then the second one. Figure IV.2 presents the variation of air temperature along the double-pass collector. In this case, we have fixed the time at noon ($I_t=850 \text{ W/m}^2$ and $T_{amb} = 35^\circ\text{C}$) to plot the spatial evolution of the air temperature through the collector's duct. The x-axis represents the position along the collector in meters (m), while the y-axis shows the temperature of the fluid in degrees Celsius ($^\circ\text{C}$). Two temperature profiles are plotted, T_{f1} and T_{f2} which represent the temperature of the fluid in the first and second pass, respectively.

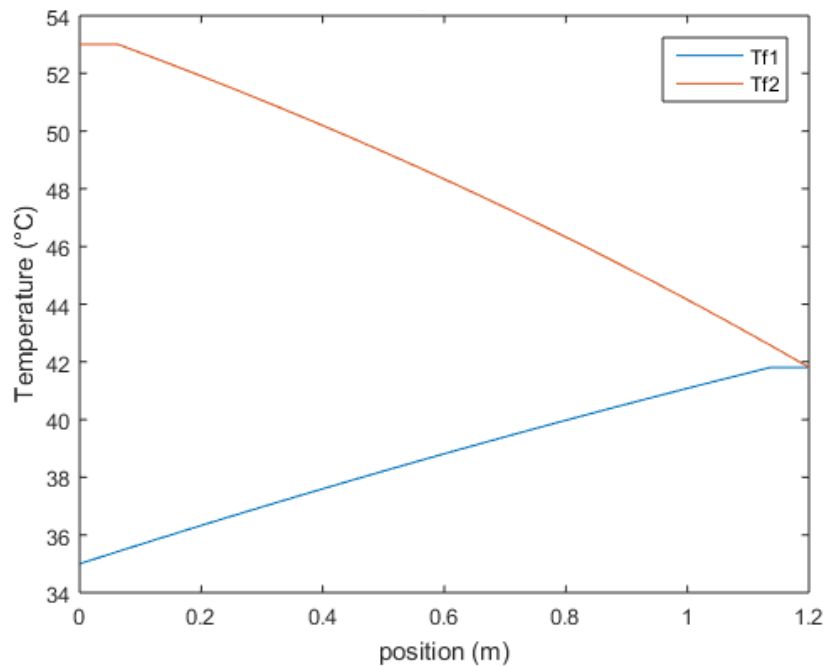


Figure IV.2 variation of fluid temperature along a double-pass collector.

Initially, in the first pass, the air absorbs heat as it flows through the collector, warmed by the absorber surface and solar radiation and reaches a maximum of 41°C . After passing through this first section, the air enters the second pass, where it continues to be heated. The second pass provides an additional opportunity for heat transfer, as the air comes into contact with the absorber surface once again, the maximum temperature of air is recorded at the outlet (53°C), this corresponds to an approximate temperature increase of 29.27%, representing a significant improvement in thermal performance. The design of this collector allows for improved thermal

performance because the air spends more time in the collector, thereby enhancing heat transfer efficiency making it more effective in capturing and utilizing solar energy.

IV.4. Effect of mass flow rate on fluid temperatures as a function of distance:

Figure IV.3 illustrates the effect of mass flow rate on the spacial variation of fluid temperatures for different mass flow values, $mf=[0.01,0.02,0.03]$ kg/s. The same pattern is observed across all three values: the air first heats up in the first pass and continues to warm in the second pass. The air temperature reaches a maximum of 50°C, 52°C, and 57°C at the outlet for mass flow rates of 0.03 kg/s, 0.02 kg/s, and 0.01 kg/s, respectively. It is also observed that an increase in flow rate causes a reduction in the temperature difference between the collector's inlet and outlet. This behaviour can be explained by the amount of fluid flow.

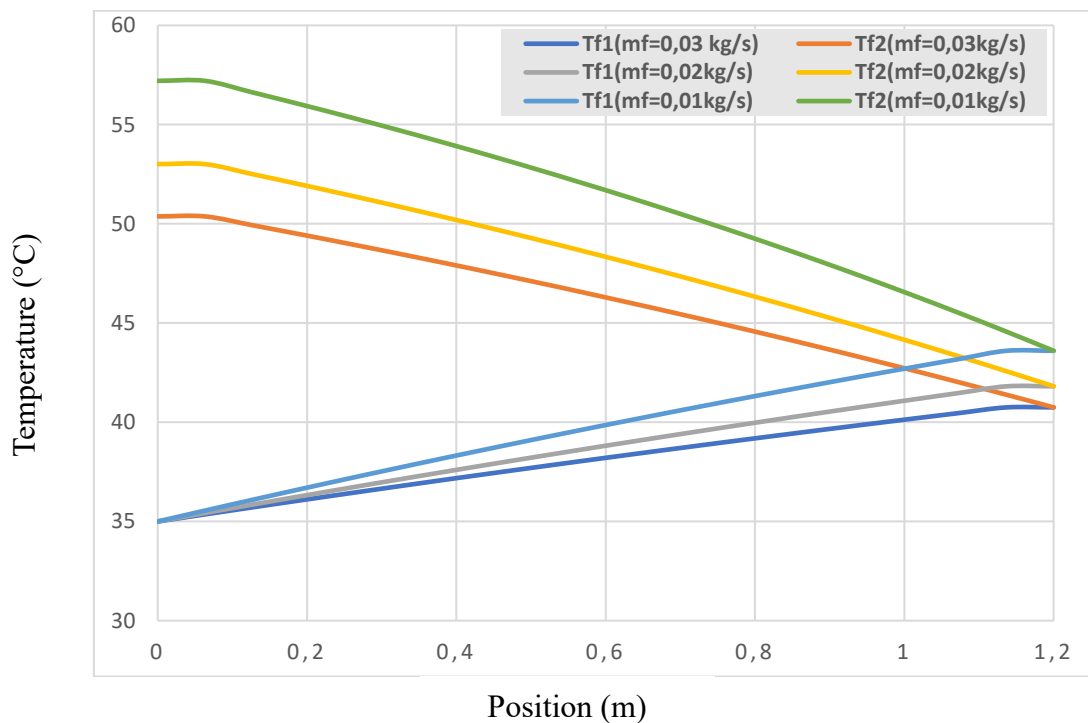


Figure IV.3:the effect of mass flow rate on the variation of fluid temperatures with different values of masse flow mf [0,01 0,02 0,03 kg/s]

A higher mass flow rate increases the volume of fluid passing through the collector per unit of time, leading to a decrease in the residence time of the fluid in both channels and therefore a smaller temperature rise. This occurs because the absorbed energy is distributed over a larger mass of fluid, which slows the rate of heating. Conversely, a lower mass flow rate allows the fluid to remain in the collector for a longer duration, providing more time to absorb heat. As a result, the temperature increases more significantly as the fluid absorbs more energy before exiting the collector.

IV.5. Effect of solar radiation on fluid temperatures as a function of distance

Figure IV.4 illustrates the influence of solar radiation on the spatial variation of fluid temperatures for different maximum solar intensities, corresponding to different months of the year, with values of $I_t = [700, 850, 1000]. \text{W/m}^2$

Results demonstrated a direct correlation between the increase in solar radiation intensity and the rise in fluid temperature, as the solar radiation intensity increased from 700 W/m^2 to 850 W/m^2 and then to 1000 W/m^2 , the outlet temperature for the second pass raised progressively from 50°C to 55°C , and ultimately to 60°C . Higher solar radiation intensity increases the amount of thermal energy absorbed by the absorber surface of the collector, causing a more significant rise in the fluid temperature in both the upper and lower channels. Consequently, the temperature difference of the fluid between the inlet and the outlet of the solar collector also increases. On the other hand, lower solar radiation intensity reduces the energy available for absorption, leading to a smaller increase in the fluid's temperature.

Solar radiation intensity plays a critical role in determining the fluid temperature profile within a solar collector. Higher radiation levels enable more efficient heating and create steeper temperature gradients, thereby optimizing system performance. Understanding and accounting for these variations is essential for the effective design and operation of solar thermal systems.

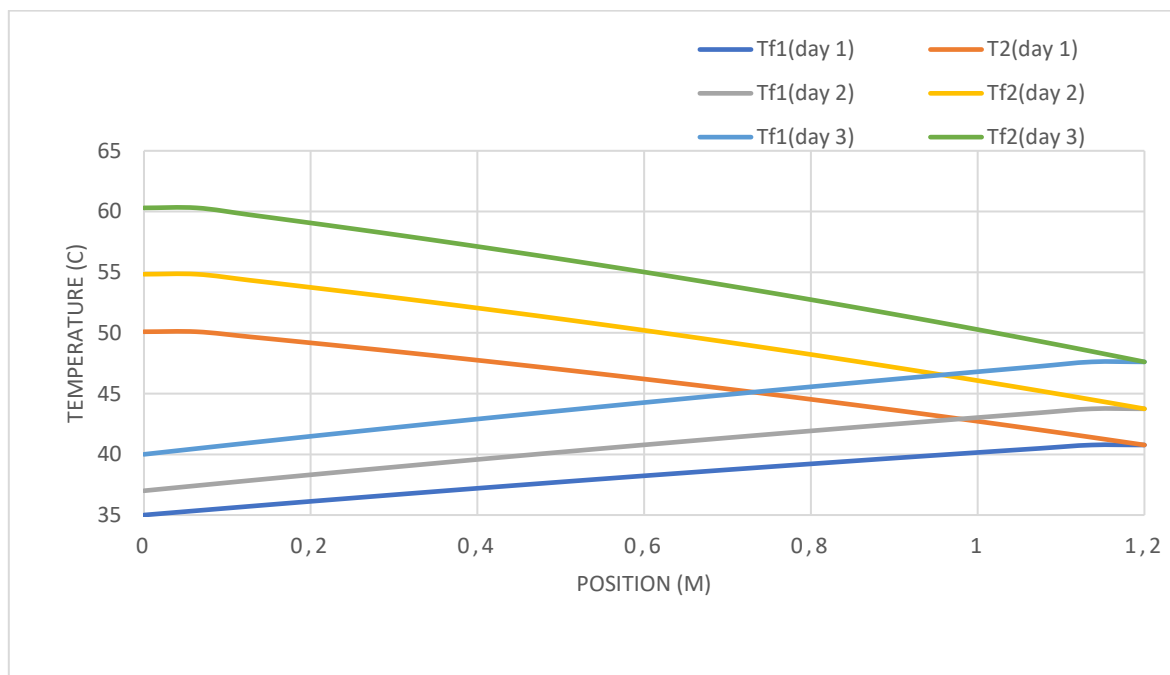


Figure IV.4: The effect of solar radiation on the variation of fluid temperatures with different values of solar radiation $I_t [700 \ 850 \ 1000]$

IV.6. Effect of Mass Flow Rate and Solar Radiation on Fluid Temperatures as a Function of Time

IV.6.1. Effect of mass flow rate

Figure IV.5 illustrates the impact of the mass flow rate on the outlet fluid temperature in a solar collector, as a function of time for three values of mass flow rates: 0.03kg/s, 0.02kg/s and 0.01 kg/s.

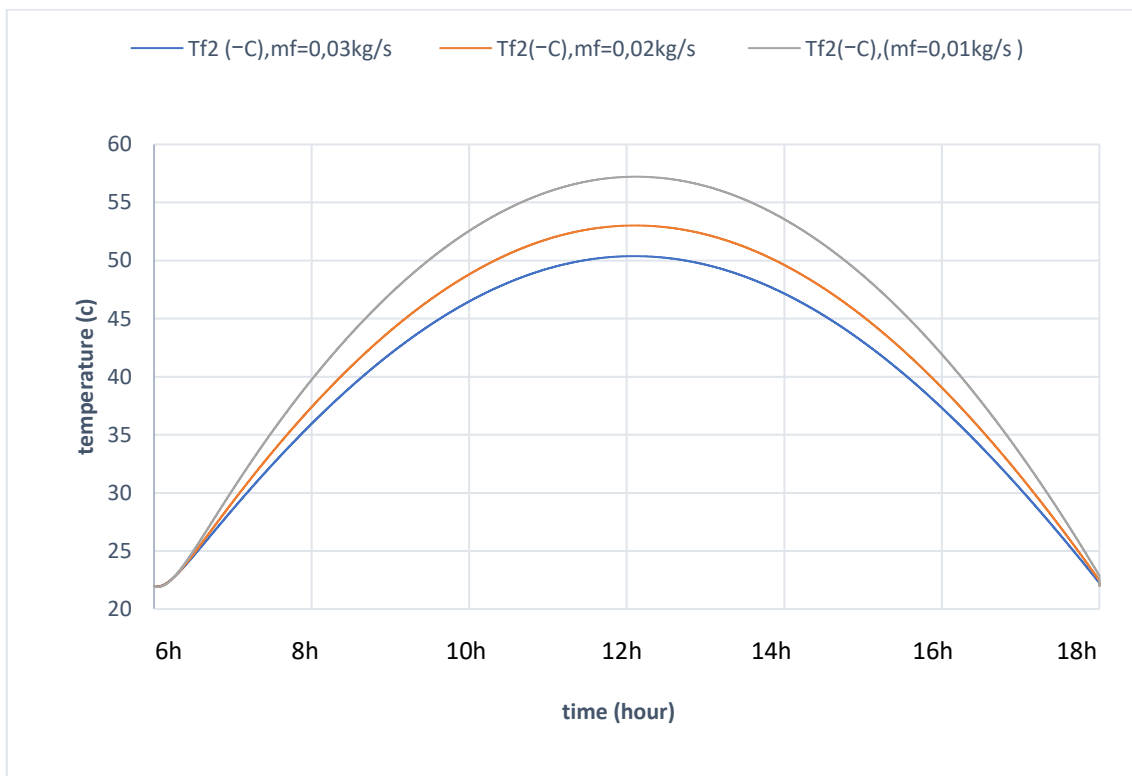


Figure IV.5:the impact of the mass flow rate on the outlet fluid temperature in a solar collector

The thermal behaviour of the solar collector over time can be divided into three distinct phases. During the rising phase (6h to 12h) the outlet temperature progressively increases for all tested flow rates, directly correlating with the rising solar radiation intensity in the morning. In the peak phase (around 12h), the outlet temperatures reach their maximum values (50°C, 53°C and 57°C) respectively, coinciding with the peak solar radiation intensity. Finally, during the falling phase (12h to 18h), the outlet temperatures decline across all flow rates as the solar radiation intensity decreases in the afternoon. Despite the similar overall downward trends, the temperature differences caused by varying mass flow rates persist, underlining the continued influence of flow rate on thermal performance throughout the entire cycle.

$m_f = 0.03$ kg/s demonstrated the lowest outlet temperature among the tested flow rates. This outcome can be attributed to the higher mass flow rate, which reduces the residence time of the fluid within the solar collector. As the fluid moves more rapidly through the system, its capacity to absorb and retain heat is limited, resulting in a lower temperature rise. In contrast, ($m_f = 0.02$ kg/s) exhibited slightly higher outlet temperatures due to the moderate flow rate, which allows for a balance between residence time and heat absorption. Finally, ($m_f = 0.01$ kg/s) recorded the highest outlet temperature. The lower mass flow rate enabled the fluid to move more slowly through the collector, thereby increasing the residence time and maximizing heat transfer. These observations highlight the critical influence of mass flow rate on the thermal performance of solar collectors, where slower flow rates enhance heat absorption and lead to higher outlet fluid temperature.

IV.6.2. Effect of solar intensity

The variation in solar intensity directly impacts the performance of a solar collector. To analyze the effect of daily solar intensity fluctuations on the outlet air temperature of the collector, we have tested three different days representing various months of the year (Figure IV.6) .

- *day 1* → Maximum $I_t = 700$ w/m² (june)
- *day 2* → Maximum $I_t = 850$ w/m² (september)
- *day 3* → Maximum $I_t = 1000$ w/ m² (april)

By examining these variations, we can better understand how changes in solar intensity throughout the day and across different seasons influence the thermal efficiency and overall performance of the solar collector.

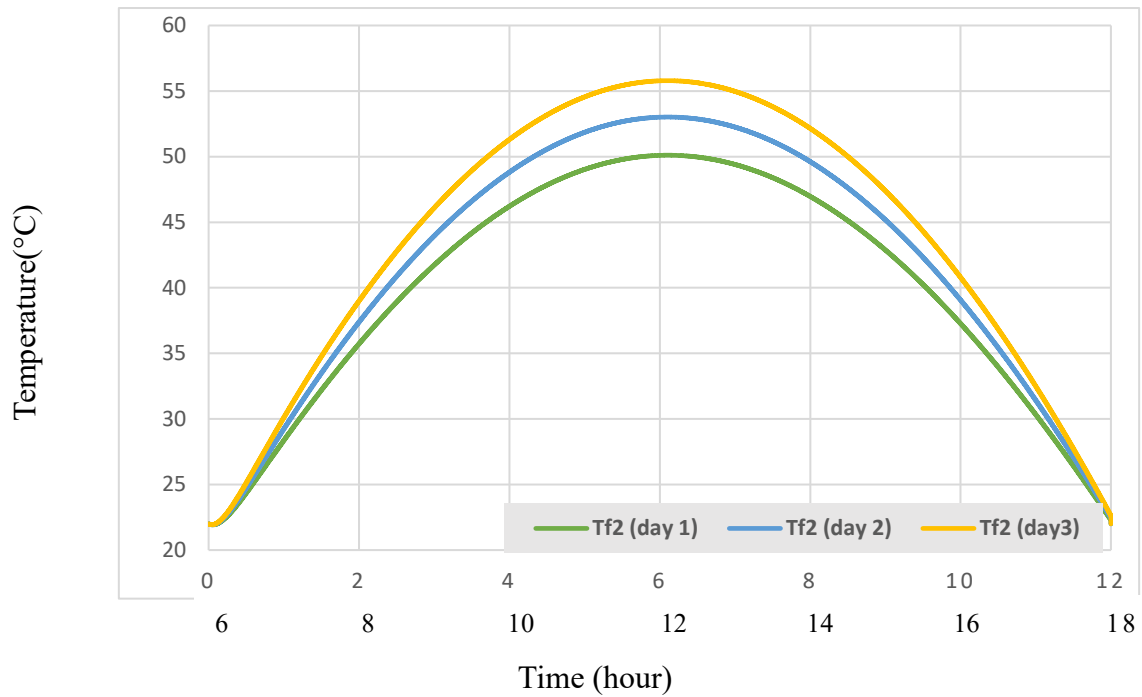


Figure IV.6:The impact of solar intensity on the outlet temperature of the fluid in a solar collector

The outlet air temperature of the collector over the three days is primarily influenced by solar radiation. All three curves display a similar pattern, characterized by a steady rise throughout the day, followed by a gradual decline towards the end of the day.

As solar radiation increases, the outlet temperature rises proportionally. This behaviour can be attributed to the greater amount of solar energy being absorbed by the collector surface at higher radiation intensities. Consequently, more heat is transferred to the fluid circulating within the system. Specifically, during peak radiation hours, the solar collector absorbs maximum thermal energy, allowing for an enhanced heat exchange process and resulting in a significant rise in the outlet temperature. During periods of lower radiation intensity, such as early morning or late afternoon, the thermal energy input decreases, limiting the temperature increase of the fluid. This trend highlights the role of solar radiation in driving the thermal performance of solar collectors and influencing the overall temperature behaviour of the working fluid.

In addition to analysing the effect of solar radiation intensity on outlet fluid temperature, we also examined its behaviour over different days where peak solar intensities varied between 700 W/m², 850 W/m², and 1000 W/m². The results clearly demonstrated that higher peak solar intensities corresponded to greater outlet temperatures. For instance, at 700 W/m², the outlet temperature reached 50°C, whereas at 850 W/m² and 1000 W/m² the temperature rise became more pronounced, reaching 53°C and 56°C, respectively, reflecting the increased energy absorbed by the collector. This correlation can be explained by the fact that higher solar

intensity enhances the thermal energy available for transfer, resulting in a more significant temperature elevation of the working fluid. These findings emphasize the critical role of solar radiation variability in determining the thermal performance of the solar collector system, particularly as the peak intensity governs the maximum temperature achievable.

IV.7. Thermal efficiency

The energy efficiency of a solar collector is defined as the ratio of the useful energy collected by the solar collector to the total energy received from the sun. This parameter is often used to assess the viability and efficiency of the energy conversion and utilization system. the corresponding equation is given by:

$$\eta = \frac{Q_u}{Q_{tot}} \quad \text{IV.1}$$

or

$$\eta = \frac{\dot{m} C_p \Delta T}{I_t A_c} \quad \text{IV.2}$$

where

\dot{m} : Mass flow rate of the working fluid (kg/s).

C_p : Specific heat capacity of the fluid (J/(kg·K)).

ΔT :temperature difference between the entry and exit of the collector ($T_{f2 \text{ out}} - T_{f1 \text{ in}}$).

I_t :solar radiation (w/m²).

A_c :surface of the collector(m²)

IV.7.1. Temporal Variation of Thermal Efficiency

Figure IV.7 illustrates the change in thermal efficiency of a system over time during a given period, ranging from 10:00 AM to 6:00 PM for a maximal solar intensity of 850 (w/m²) and mass flow $m_f=0.01$ (kg/ s).

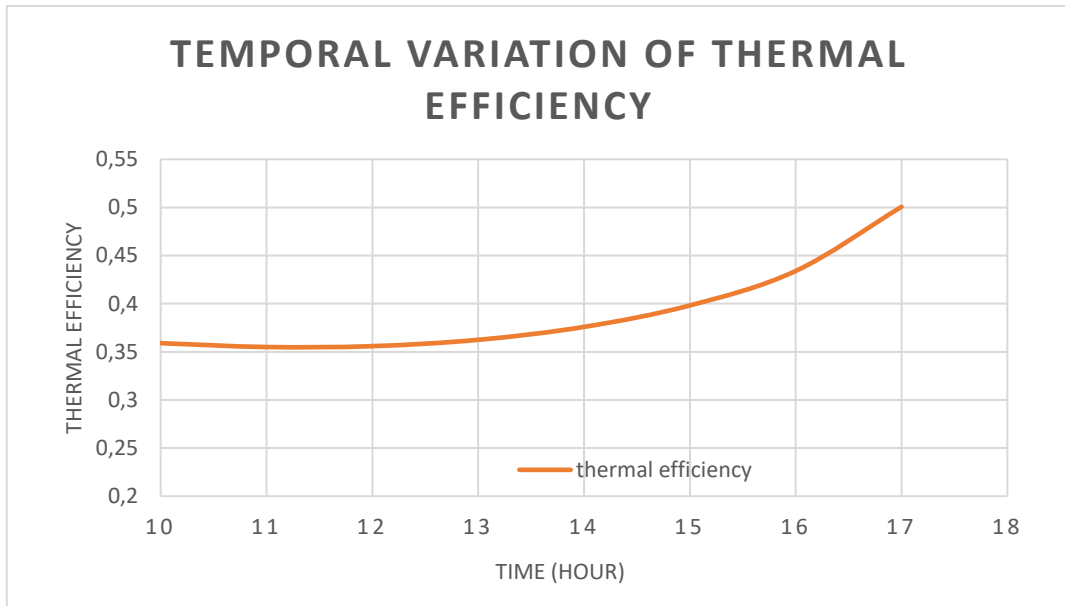


Figure IV.7:Temporal Variation of Thermal Efficiency

Thermal efficiency is directly influenced by solar intensity; however, this relationship is moderated by thermal losses and the system's operating conditions. Higher solar intensity generally enhances thermal efficiency, provided that losses are minimized through effective insulation and the use of materials with high absorptive capacity.

The figure shows a clear increase in efficiency throughout the day going from 35% in the morning to 50% in the evening ,this can be explained by the nature of the mathematical model and the efficiency equation because as we approach sunset values of radiation tends toward zero, which causes the efficiency to increase.

IV.7.2. Impact of mass flow rate on thermal efficiency

Figure IV.7 shows the effect of mass flow rate on thermal efficiency of a double pass solar collector, various values of mass flow were tested (going from 0.005 kg/s to 0.03 kg/s).

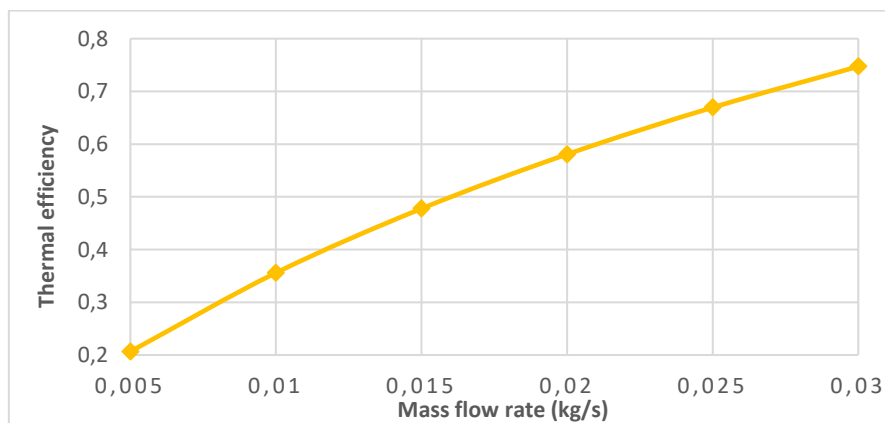


Figure IV.8:impact of mass flow rate on thermal efficiency

It is observed that the thermal efficiency of the collector increases with the air flow rate circulating through both passes, indicating that higher mass flow rates enhance convective heat transfer, allowing more energy to be extracted from the solar collector's surface and improving overall performance. The thermal energy collected increases with the mass flow rate, as it is directly proportional to it. There is a clear positive correlation between mass flow rate and thermal efficiency, with the latter steadily rising as the flow rate increases, reaching 75%. However, once the mass flow rate exceeds 0.02 kg/s, efficiency continues to rise but at a much slower rate, suggesting the system is approaching its maximum efficiency or saturation point. This is because, at higher flow rates, the fluid moves more rapidly through the collector, reducing its residence time and, consequently, its ability to absorb heat from the absorber. Although thermal losses are minimized as the fluid passes through more quickly, the overall efficiency cannot increase indefinitely due to the limitations in heat transfer at higher flow rates. In contrast, at lower flow rates, the fluid stays longer within the collector improving heat exchange. However, this results in a higher average fluid temperature, leading to increased thermal losses through convection and radiation to the environment, which reduces efficiency. Therefore, a balance is required between maximizing efficiency and achieving the desired fluid temperature.

IV.7.3. Impact of solar intensity on thermal efficiency

Figure IV.8 illustrates impact of solar intensity on thermal efficiency showing a clear upward trend. As solar intensity increases from 700 to 1100 W/m², the thermal efficiency steadily improves.

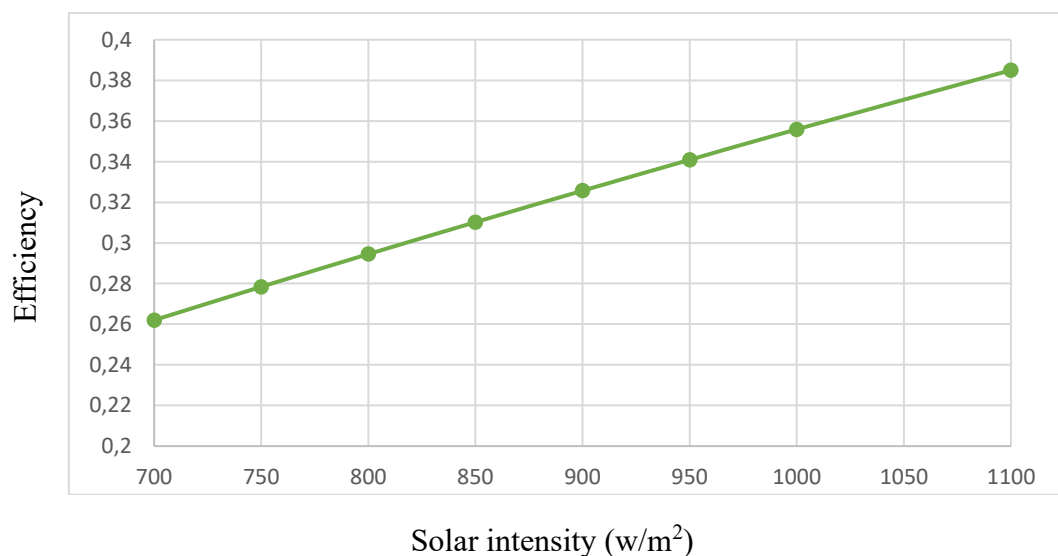


Figure IV.9: impact of solar radiation on thermal efficiency

This positive correlation highlights that higher solar intensities provide more energy input to the system, enhancing the thermal performance of the solar collector. This indicates that the collector operates more efficiently under higher irradiance levels, taking full advantage of the increased solar resource. We can see that the efficiency is relatively lower, reaching a maximum of 38% because the efficiency is inversely proportional to the radiation.

IV.7.4. Conclusion

In this chapter, we have explored the results of the simulation using MATLAB. The results obtained demonstrate the influence of mass flow rate and solar intensity on fluid temperatures and the thermal efficiency of a solar collector. Increasing the mass flow rate enhances thermal efficiency due to improved convective heat transfer. Similarly, higher solar intensities result in a steady increase in thermal efficiency, reflecting the system's ability to effectively convert greater solar energy inputs into useful thermal energy. Together, these results highlight the critical role of optimizing both operational parameters to achieve maximum efficiency.

IV.8. General conclusion :

This thesis highlights the crucial importance of solar collectors in the pursuit of sustainable energy solutions, particularly in applications requiring thermal energy. Among these, solar air heaters represent an efficient and environmentally friendly method for harnessing solar radiation to meet heating demands in various sectors. This study focuses on the thermal analysis of a flat plate solar air heater, employing energy balance equations and numerical simulations to optimize its performance. The work aims to provide valuable insights into the design and operational parameters affecting its efficiency.

In the first part, we conducted a theoretical study of the system using energy balance equations, deriving specific equations for each component of the solar collector. This analysis included the insulation, the absorber, the working fluid in the double-pass configuration, and the glass cover, providing a comprehensive understanding of the thermal behavior of each element.

In the second part, we developed a MATLAB code to numerically solve the energy balance equations using the simple iterative method. After analysis, the following observations can be concluded.

The results revealed that both the mass flow rate and solar radiation significantly influence the fluid temperature exiting the solar collector.

- a lower mass flow rate allows the fluid to stay in the collector for a longer period, which enables it to absorb more heat. This leads to a greater temperature increase along the length of the collector.
- Higher radiation levels enable more efficient heating and create steeper temperature gradients, causing a more significant rise in the fluid temperature as it passes through the system.(up to 60 °c).

Moreover, The thermal efficiency of a solar collector is influenced by the impact of mass flow rate and solar intensity. An increase in mass flow rate improves thermal efficiency by enhancing convective heat transfer. Likewise, greater solar intensities lead to a consistent rise in thermal efficiency, showcasing the system's capability to efficiently transform higher solar energy inputs into usable thermal energy. Adjusting the mass flow rate within an optimal range is essential to balance efficiency improvements with energy consumption and system constraints.

This study provides a foundation for further exploration and optimization of solar air heaters. Future research could focus on integrating advanced materials, such as phase change materials, to enhance thermal storage and improve efficiency during nighttime operation. Additionally, implementing optimization algorithms could help identify the ideal design parameters, such as the size of the air inlet or the geometry of the absorber, to maximize performance. Experimental validation of the numerical results under varying climatic conditions would strengthen the reliability of the findings. Moreover, extending the study to hybrid systems combining solar air heaters with other renewable technologies could provide innovative solutions for sustainable energy applications. Finally, exploring the economic feasibility and scalability of these systems for industrial and domestic uses could promote their adoption globally.

References

Chapter I

- [1] World Meteorological Organization. (2023, October 25). Greenhouse gas concentrations surge again to new record in 2023
- [2] Kamarulzaman, A., Hasanuzzaman, M., & Rahim, N. A. (2021). Global advancement of solar drying technologies and its future prospects: A review. *Solar Energy*, 221, 559–582.
- [3] Yahiaoui, L. Z. E. L. (2020). Conception et réalisation d'un capteur solaire plan à air [Mémoire de master, Université de Bouira].
- [4] Mohana, Y., Mohanapriya, R., Anukiruthika, T., et al. (2020). Solar dryers for food applications: Concepts, designs, and recent advances. *Solar Energy*, 208, 321–344.
- [5] Tiwari, A. (2016). A review on solar drying of agricultural produce. *Journal of Food Processing & Technology*, 7(9), 1–12.
- [6] Benatiallah, D. (2014). Étude et simulation de flux solaire avec intégration d'un système d'information géographique (SIG) pour la wilaya d'Adrar [Mémoire de magistère, Université Ahmed Draia, Adrar].
- [7] Benatiallah, D. (2019). Détermination du gisement solaire par imagerie satellitaire avec intégration dans un système d'information géographique pour le sud de l'Algérie [Thèse de doctorat, Université Ahmed Draia, Adrar].
- [8] Ministère de l'Énergie. (2019). Bilan énergétique national.
- [9] Holman, J. P. (2010). *Heat transfer* (10th ed.). McGraw-Hill
- [10] Bejan, A. (2013). *Convection heat transfer*. John Wiley & Sons.
- [11] Bencherif, L., Boussoukaia, T., et al. (2018). Effet du modèle double vitrage sur les performances d'un capteur solaire [Thèse de doctorat, Université Ahmed Draia, Adrar].
- [12] Taleb, M. H. A., Zenatti, A., & Benzenine, H. (2022). Capteur solaire en présence d'un absorbeur muni d'ailettes longitudinales [Thèse de doctorat].
- [13] Hammoumi, M., & Morghad, H. (2013). Étude expérimentale d'un capteur solaire plan à air spécifique au séchage [Mémoire de master, Université de Tlemcen].
- [14] Slimane, S. (2019). Étude du comportement thermique et dynamique d'un capteur solaire plan à air en présence de chicanes transversales [Thèse de doctorat, Université Ibn Khaldoun, Tiaret].
- [15] Reggadi, E. (2018). Étude de l'influence du matériau de l'absorbeur sur le comportement thermique d'un capteur solaire plan à air à double passe [Thèse de doctorat, Université Ibn Khaldoun, Tiaret].
- [16] Noun, M. (2018). Étude des paramètres impactant sur le rendement d'un capteur solaire [Mémoire de master, Université de Annaba].

[17] Hadj Ammar, M. A. (2009). Impact de l'écart de température entre l'absorbeur et la vitre sur l'efficacité du capteur solaire à double vitrage [Thèse de magistère, Université Kasdi Merbah, Ouargla].

[18] Ferdjani, A. T. (2013). Développement d'un logiciel de simulation des performances thermiques des capteurs solaires plans [Thèse de doctorat].

[19] Yahiaoui, L. Z. E. L. (2020). Conception et réalisation d'un capteur solaire plan à air [Mémoire de master, Université de Bouira].

[20] Kumar, R., & Rosen, M. A. (2011). A critical review of photovoltaic–thermal solar collectors for air heating. *Applied Energy*, 88(11), 3603–3614.

[21] Taleb, M. H. A., Zenatti, A., & Benzenine, H. (2022). Capteur solaire en présence d'un absorbeur muni d'ailettes longitudinales [Thèse de doctorat].

[22] Kalogirou, S. A. (2004). Solar thermal collectors and applications. *Progress in energy and combustion science*, 30(3), 231-295.

Chapter II

[1] Daliran, A., & Ajabshirchi, Y. (2018). Theoretical and experimental research on effect of fins attachment on operating parameters and thermal efficiency of solar air collector. *Information processing in agriculture*, 5(4), 411-421..

[2] Karim, M. A., Perez, E., & Amin, Z. M. (2014). Mathematical modelling of counter flow v-groove solar air collector. *Renewable energy*, 67, 192-201. [4] Kumar, R., & Chand, P. (2017). Performance enhancement of solar air heater using herringbone corrugated fins. *Energy*, 127, 271-279.

[5] Singh, S., & Dhiman, P. (2016). Thermal and thermohydraulic efficiency of recyclic-type double-pass solar air heaters with fins and baffles. *Heat Transfer Engineering*, 37(15), 1302-1317.

[6] Abo-Elfadl, S., Hassan, H., & El-Dosoky, M. F. (2020). Study of the performance of double pass solar air heater of a new designed absorber: An experimental work. *Solar Energy*, 198, 479-489.

[7] Al-Neama, M. A., & Farkas, I. (2019). Thermal efficiency of vertical and horizontal-finned solar collector integrated with forced air circulation dryer for Apple as a sample. *Drying Technology*, 37(5), 546-558.

[8] Singh, S., & Dhiman, P. (2016). Thermal and thermohydraulic efficiency of recyclic-type double-pass solar air heaters with fins and baffles. *Heat Transfer Engineering*, 37(15), 1302-1317.

[9] Khanlari, A., Güler, H. Ö., Tuncer, A. D., Şirin, C., Bilge, Y. C., Yılmaz, Y., & Güngör, A. (2020). Experimental and numerical study of the effect of integrating plus-shaped perforated baffles to solar air collector in drying application. *Renewable energy*, 145, 1677-1692.

- [10] Garcia, R. P., del Rio Oliveira, S., & Scalon, V. L. (2019). Thermal efficiency experimental evaluation of solar flat plate collectors when introducing convective barriers. *Solar Energy*, 182, 278-285.
- [11] Hassan, H., Abo-Elfadl, S., & El-Dosoky, M. F. (2020). An experimental investigation of the performance of new design of solar air heater (tubular). *Renewable Energy*, 151, 1055-1066.
- [12] Ramesh, C., Vijayakumar, M., Alshahrani, S., Navaneethakrishnan, G., Palanisamy, R., Saleel, C. A., ... & Panchal, H. (2022). Performance enhancement of selective layer coated on solar absorber panel with reflector for water heater by response surface method: A case
- [13] Singh, A. P., & Singh, O. P. (2020). Curved vs. flat solar air heater: Performance evaluation under diverse environmental conditions. *Renewable Energy*, 145, 2056-2073.
- [14] Nadir, N., Bouguettaia, H., Boughali, S., & Bechki, D. (2019). Use of a new agricultural product as thermal insulation for solar collector. *Renewable Energy*, 134, 569-578.
- [15] Moradi, R., Kianifar, A., & Wongwises, S. (2017). Optimization of a solar air heater with phase change materials: Experimental and numerical study. *Experimental Thermal and Fluid Science*, 89, 41-49.
- [16] Vijayan, S., Arjunan, T. V., & Kumar, A. (2020). Exergo-environmental analysis of an indirect forced convection solar dryer for drying bitter gourd slices. *Renewable Energy*, 146, 2210-2223.
- [17] ElGamal, R., Kishk, S., Al-Rejaie, S., & ElMasry, G. (2021). Incorporation of a solar tracking system for enhancing the performance of solar air heaters in drying apple slices. *Renewable Energy*, 167, 676-684.